Studying double charm decays of $B_{u,d}$ and B_s mesons in the MSSM with R-parity violation

C. S. Kim,[1,*] Ru-Min Wang,[1,†] and Ya-Dong Yang[2,‡]

[1]*Department of Physics and IPAP, Yonsei University, Seoul 120-479, Korea*
[2]*Institute of Particle Physics, Huazhong Normal University, Wuhan 430070, People's Republic of China*
(Received 29 December 2008; published 5 March 2009)

Motivated by the possible large direct CP asymmetry of $\bar{B}_d^0 \to D^+D^-$ decays measured by the Belle Collaboration, we investigate double charm $B_{u,d}$ and B_s decays in the minimal supersymmetric standard model with R-parity violation. We derive the bounds on relevant R-parity violating couplings from the current experimental data, which show quite consistent measurements among relative collaborations. Using the constrained parameter spaces, we explore R-parity violating effects on other observables in these decays, which have not been measured or have not been well measured yet. We find that the R-parity violating effects on the mixing-induced CP asymmetries of $\bar{B}_d^0 \to D^{(*)+}D^{(*)-}$ and $\bar{B}_s^0 \to D_s^{(*)+}D_s^{(*)-}$ decays could be very large; nevertheless, the R-parity violating effects on the direct CP asymmetries could not be large enough to explain the large direct CP violation of $\bar{B}_d^0 \to D^+D^-$ from Belle. Our results could be used to probe R-parity violating effects and will correlate with searches for direct R-parity violating signals in future experiments.

DOI: 10.1103/PhysRevD.79.055004 PACS numbers: 12.60.Jv, 12.15.Ji, 13.25.Hw, 14.40.Lb

I. INTRODUCTION

Double charm decays of $B_{u,d}$ and B_s provide us with a rich field to study CP violation and final-state interactions as well as to extract information from Cabibbo-Kobayashi-Maskawa (CKM) elements. CP asymmetries (CPAs) in these decays play an important role in testing the standard model (SM) as well as in exploring new physics (NP) [1,2].

Double charm decays, $\bar{B}_d^0 \to D^{(*)+}D^{(*)-}$, $B_u^- \to D^{(*)0}D^{(*)-}$, and $\bar{B}_s^0 \to D_s^{(*)+}D^{(*)-}$, are dominated by color-allowed tree $b \to c\bar{c}d$ transitions, but involve small penguin pollution from $b \to u\bar{u}d$ transitions carrying a different weak phase. The latter contributions lead to direct CPAs, which are very small (about the order of 10^{-2}) in the SM. If penguin corrections are neglected, the SM predictions for the direct CPAs would be zero. It is interesting to note that both *BABAR* and Belle have measured the direct CPA in $B_d^0 \to D^+D^-$ decay,

$$\mathcal{C}(B_d^0, \bar{B}_d^0 \to D^+D^-) = \begin{cases} -0.91 \pm 0.23 \pm 0.06 & (\text{Belle}\,[3]) \\ -0.07 \pm 0.23 \pm 0.03 & (BABAR\,[4]), \end{cases} \tag{1}$$

respectively. One would find that the difference between the two measurements is

$$\Delta\mathcal{C} = 0.84 \pm 0.32; \tag{2}$$

i.e., the difference is as large as 2.7σ. So far, such a large direct CPA has not been observed in the other measurements of $\bar{B}_d^0 \to D^{(*)+}D^{(*)-}$, $B_u^- \to D^{(*)0}D^{(*)-}$, and $\bar{B}_s^0 \to D_s^{(*)+}D^{(*)-}$ decays [4–11], which involve the same quark-level weak decays. If the large CP violation in $\bar{B}_d^0 \to D^+D^-$ from Belle is true, it would establish the presence of NP. At present, one cannot conclude that NP is present in those decays. Equivalently, one cannot assume that the CPAs are in agreement with the SM expectations either. Recently, the large direct CPA in $\bar{B}_d^0 \to D^+D^-$ has been investigated with possible NP scenarios, such as unparticle interaction [12] and the NP effects in the electroweak penguin sector [13,14], and so on.

In this paper, we would like to investigate $B_{u,d}$ and B_s double charm decays systematically in the minimal supersymmetric standard model (MSSM) [15,16] with R-parity violation [17,18]. In the literature, the possible appearance of the R-parity violating (RPV) couplings [17,18], which violate the lepton and/or baryon number conservations, has gained full attention in searching for supersymmetry [19,20]. The effects of supersymmetry with R-parity violation in B meson decays have been extensively investigated, for instance, in Refs. [21–24]. In our work, 24 double charm decays $\bar{B}_d^0 \to D^{(*)+}D_{(s)}^{(*)-}$, $\bar{B}_u^- \to D^{(*)0}D_{(s)}^{(*)-}$, and $\bar{B}_s^0 \to D_s^{(*)+}D_{(s)}^{(*)-}$ are studied in the RPV MSSM. For simplicity, we employ naive factorization [25] for the hadronic dynamics, which is expected to be reliable for the color-allowed amplitudes, which are dominant contributions in those double charm decays.

The color-allowed tree-level-dominated decays of $b \to c\bar{c}d$, i.e. $\bar{B}_d^0 \to D^{(*)+}D^{(*)-}$, $B_u^- \to D^{(*)0}D^{(*)-}$, and $\bar{B}_s^0 \to D_s^{(*)+}D^{(*)-}$, involve the same set of RPV coupling constants. For these processes, besides the CPA in $\bar{B}_d^0 \to D^+D^-$, a few other observables in $B_{u,d} \to D^{(*)}D^{(*)}$ have already been measured by the *BABAR* and Belle collaborations [4–11,3,26]. To derive constraints on the relevant RPV couplings, we will choose a set of data from the aforementioned measurements which have quite high con-

*cskim@yonsei.ac.kr
†ruminwang@cskim.yonsei.ac.kr
‡yangyd@iopp.ccnu.edu.cn

sistency between the measurements of *BABAR* and Belle. Then, using the constrained RPV coupling parameter spaces, we predict the RPV effects on the other observables in $\bar{B}_d^0 \to D^{(*)+}D^{(*)-}$, $B_u^- \to D^{(*)0}D^{(*)-}$, and $\bar{B}_s^0 \to D_s^{(*)+}D^{(*)-}$ decays, whose measurements from *BABAR* and Belle are not compatible within the 2σ error range, and/or which have not been measured yet. One of our goals is to see how large the direct CPA of $\bar{B}_d^0 \to D^+D^-$ can be within the constrained parameter spaces. We find that the lower limit of $\mathcal{C}(B_d^0, \bar{B}_d^0 \to D^+D^-)$ could be just slightly decreased by the RPV couplings, and the RPV effects on this quantity are not large enough to explain the large direct CP violation from Belle, although the mixing-induced CPAs of $\bar{B}_d^0 \to D^{(*)+}D^{(*)-}$ are very sensitive to the RPV couplings.

The decays $\bar{B}_d^0 \to D^{(*)+}D_s^{(*)-}$, $B_u^- \to D^{(*)0}D_s^{(*)-}$, and $\bar{B}_s^0 \to D_s^{(*)+}D_s^{(*)-}$ are governed by the $b \to c\bar{c}s$ transition at the quark level, and also involve the same set of RPV coupling constants. They have similar properties to $\bar{B}_d^0 \to D^{(*)+}D^{(*)-}$, $B_u^- \to D^{(*)0}D^{(*)-}$, and $\bar{B}_s^0 \to D_s^{(*)+}D^{(*)-}$ decays; nevertheless, the penguin effects are less Cabibbo suppressed. For these decays, most branching ratios and one longitudinal polarization have been measured [27–34]. We will take the same strategy as the one for $b \to c\bar{c}d$ decays to constrain relevant RPV couplings and estimate RPV effects in these decays. We find that RPV couplings could significantly affect the CPAs of these decays, and could flip their signs.

Our paper is organized as follows: In Sec. II, we briefly introduce the theoretical framework for the double charm $B_{u,d}$ and B_s decays in the RPV MSSM, and we tabulate all the theoretical input parameters. In Sec. III, we deal with the numerical results and our discussions. At first, we give the SM predictions with full uncertainties of the input parameters. Then, we derive the constrained parameter spaces which satisfy all the experimental data with high consistency between different collaborations. Finally, we predict the RPV effects on other quantities, which have not been measured or have not been well measured yet. Section IV contains our summary.

II. THEORETICAL FRAMEWORK

A. Decay amplitudes in the SM

In the SM, the low energy effective Hamiltonian for the $\Delta B = 1$ transition at a scale μ is given by [35]

$$\mathcal{H}_{\rm eff}^{\rm SM} = \frac{G_F}{\sqrt{2}} \sum_{p=u,c} \lambda_p \Big\{ C_1 Q_1^p + C_2 Q_2^p + \sum_{i=3}^{10} C_i Q_i + C_{7\gamma} Q_{7\gamma} + C_{8g} Q_{8g} \Big\} + \text{H.c.}, \tag{3}$$

where $\lambda_p = V_{pb} V_{pq}^*$ for the $b \to q$ transition ($p \in \{u, c\}$, $q \in \{d, s\}$). The detailed definition of the effective Hamiltonian can be found in [35].

It is empirically observed that naive factorization [25] still works reasonably well in the color-allowed double charm $B_{u,d}$ and B_s decay processes. We will describe the $B \to D^{(*)}D_q^{(*)}$ decay amplitudes within the naive factorization approximation in this paper. Under the naive factorization approximation, the factorized matrix elements are given by

$$A_{[BD^{(*)},D_q^{(*)}]} \equiv \langle D_q^{(*)} | \bar{q}\gamma^\mu (1-\gamma_5) c | 0 \rangle \times \langle D^{(*)} | \bar{c}\gamma_\mu (1-\gamma_5) b | B \rangle. \tag{4}$$

Decay constants and form factors [36,37] are usually defined as

$$\langle D_q(p_{D_q}) | \bar{q}\gamma^\mu \gamma_5 c | 0 \rangle = -i f_{D_q} p_{D_q}^\mu, \tag{5}$$

$$\langle D_q^*(p_{D_q^*}) | \bar{q}\gamma^\mu c | 0 \rangle = f_{D_q^*} p_{D_q^*}^\mu, \tag{6}$$

$$\langle D(p_D) | \bar{c}\gamma_\mu b | B(p_B) \rangle = \Big[(p_B + p_D)_\mu - \frac{m_B^2 - m_D^2}{q^2} q_\mu \Big] F_1(q^2) + \frac{m_B^2 - m_D^2}{q^2} q_\mu F_0(q^2), \tag{7}$$

$$\langle D^*(p_{D^*}, \varepsilon^*) | \bar{c}\gamma_\mu b | B(p_B) \rangle = \frac{2V(q^2)}{m_B + m_{D^*}} \epsilon_{\mu\nu\alpha\beta} \varepsilon^{*\nu} p_B^\alpha p_{D^*}^\beta, \tag{8}$$

$$\begin{aligned}\langle D^*(p_{D^*}, \varepsilon^*) | \bar{c}\gamma_\mu \gamma_5 b | B(p_B) \rangle &= i \Big[\varepsilon_\mu^* (m_B + m_{D^*}) A_1(q^2) - (p_B + p_{D^*})_\mu (\varepsilon^* \cdot p_B) \\ &\quad \times \frac{A_2(q^2)}{m_B + m_{D^*}} \Big] - i q_\mu (\varepsilon^* \cdot p_B) \frac{2m_{D^*}}{q^2} [A_3(q^2) - A_0(q^2)],\end{aligned} \tag{9}$$

with $q = p_B - p_{D^{(*)}}$. Then we can express $A_{[BD^{(*)},D_q^{(*)}]}$ in terms of decay constants and form factors as follows:

$$A_{[BD^{(*)},D_q^{(*)}]}=\begin{cases} if_{D_q}(m_B^2-m_D^2)F_0(m_{D_q}^2) & (DD_q)\\ 2f_{D_q^*}m_B|p_c|F_1(m_{D_q^*}^2) & (DD_q^*)\\ -2f_{D_q}m_B|p_c|A_0(m_{D_q}^2) & (D^*D_q)\\ -if_{D_q^*}m_{D_q^*}[(\varepsilon_{D^*}^*\cdot\varepsilon_{D_q^*}^*)(m_B+m_{D^*})A_1(m_{D_q^*}^2)-(\varepsilon_{D^*}^*\cdot p_{D_q^*})(\varepsilon_{D_q^*}^*\cdot p_{D^*})\frac{2A_2(m_{D_q^*}^2)}{m_B+m_{D^*}} & \\ \quad +i\epsilon_{\mu\nu\alpha\beta}\varepsilon_{D_q^*}^{*\mu}\varepsilon_{D^*}^{*\nu}p_{D_q^*}^{\alpha}p_{D^*}^{\beta}\frac{2V(m_{D_q^*}^2)}{m_B+m_{D^*}}] & (D^*D_q^*).\end{cases} \tag{10}$$

Decays $B\to D^{(*)}D_q^{(*)}$ may occur through both tree-level and loop induced (penguin) quark diagrams, and the SM decay amplitudes within the naive factorization approximation are given as

$$\mathcal{M}^{\rm SM}(B\to D^{(*)}D_q^{(*)})=\frac{G_F}{\sqrt{2}}\bigg(\lambda_c a_1^c+\sum_{p=u,c}\lambda_p[a_4^p+a_{10}^p+\xi(a_6^p+a_8^p)]\bigg)A_{[BD^{(*)},D_q^{(*)}]}, \tag{11}$$

where the coefficients $a_i^p=(C_i+\frac{C_{i\pm1}}{N_c})+P_i^p$, with the upper (lower) sign applied when i is odd (even), and P_i^p account for penguin contractions. The factorization parameter ξ in Eq. (11) arises from the transformation of $(V-A)(V+A)$ currents into $(V-A)(V-A)$ ones for the penguin operators $Q_5,\cdots,Q_8$, and it depends on properties of the final-state mesons

$$\xi=\begin{cases}+\frac{2m_{D_q}^2}{(\bar m_c+\bar m_q)(\bar m_b-\bar m_c)} & (DD_q)\\ 0 & (DD_q^*)\\ -\frac{2m_{D_q}^2}{(\bar m_c+\bar m_q)(\bar m_b+\bar m_c)} & (D^*D_q)\\ 0 & (D^*D_q^*).\end{cases} \tag{12}$$

For the penguin contractions, we will consider not only QCD and electroweak penguin operator contributions, but also contributions from the electromagnetic and chromomagnetic dipole operators. P_i^p are given as follows:

$$\begin{aligned} P_1^c&=0,\\ P_4^p&=\frac{\alpha_s}{9\pi}\bigg\{C_1\bigg[\frac{10}{9}-G_{D_q^{(*)}}(m_p)\bigg]-2F_1C_{8g}^{\rm eff}\bigg\},\\ P_6^p&=\frac{\alpha_s}{9\pi}\bigg\{C_1\bigg[\frac{10}{9}-G_{D_q^{(*)}}(m_p)\bigg]-2F_2C_{8g}^{\rm eff}\bigg\},\\ P_8^p&=\frac{\alpha_e}{9\pi}\frac{1}{N_c}\bigg\{(C_1+N_cC_2)\bigg[\frac{10}{9}-G_{D_q^{(*)}}(m_p)\bigg]-3F_2C_{7\gamma}^{\rm eff}\bigg\},\\ P_{10}^p&=\frac{\alpha_e}{9\pi}\frac{1}{N_c}\bigg\{(C_1+N_cC_2)\bigg[\frac{10}{9}-G_{D_q^{(*)}}(m_p)\bigg]-3F_1C_{7\gamma}^{\rm eff}\bigg\},\end{aligned} \tag{13}$$

where the penguin loop-integral function $G_{D_q^{(*)}}(m_p)$ is given by

$$G_{D_q^{(*)}}(m_p)=\int_0^1 duG(m_p,k)\Phi_{D_q^{(*)}}(u), \tag{14}$$

$$G(m_p,k)=-4\int_0^1 dxx(1-x)\times\ln\bigg[\frac{m_p^2-k^2x(1-x)}{m_b^2}-i\epsilon\bigg], \tag{15}$$

with the penguin momentum transfer $k^2=m_c^2+\bar u(m_b^2-m_c^2-m_{M_2}^2)+\bar u^2m_{M_2}^2$, where $\bar u\equiv1-u$. In the function $G_{D_q^{(*)}}(m_p)$, we have used a $D_q^{(*)}$ meson-emitting distribution amplitude $\Phi_{D_q^{(*)}}(u)=6u(1-u)[1+a_{D_q^{(*)}}(1-2u)]$, instead of keeping k^2 as a free parameter as usual. The constants F_1 and F_2 in Eq. (13) are defined by

$$F_1=\begin{cases}\int_0^1du\Phi_{D_q}(u)\frac{m_b}{m_b-m_c}\frac{m_b^2-um_{D_q}^2-2m_c^2+m_bm_c}{k^2} & (DD_q)\\ \int_0^1du\Phi_{D_q^*}(u)\frac{m_b}{k^2}(\bar um_b+\frac{2um_{D_q^*}}{m_b-m_c}\epsilon_2^*\cdot p_1-um_c) & (DD_q^*)\\ \int_0^1du\Phi_{D_q}(u)\frac{m_b}{m_b+m_c}\frac{m_b^2-um_{D_q}^2-2m_c^2-m_bm_c}{k^2} & (D^*D_q)\\ \int_0^1du\Phi_{D_q^*}(u)\frac{m_b}{k^2}(\bar um_b+\frac{2um_{D_q^*}}{m_b+m_c}\epsilon_2^*\cdot p_1+um_c) & (D^*D_q^*),\end{cases} \tag{16}$$

$$F_2=\begin{cases}\int_0^1du\Phi_{D_q}(u)\frac{m_b}{k^2}[\bar u(m_b-m_c)+m_c] & (DD_q)\\ 0 & (DD_q^*)\\ \int_0^1du\Phi_{D_q}(u)\frac{m_b}{k^2}[\bar u(m_b+m_c)-m_c] & (D^*D_q)\\ 0 & (D^*D_q^*),\end{cases} \tag{17}$$

where $\epsilon_{2L}^*\cdot p_1\approx(m_b^2-m_{M_q^*}^2-m_c^2)/(2m_{M_q^*})$ and $\epsilon_{2T}^*\cdot p_1=0$ for $B\to D^*D_q^*$ decays.

B. Decay amplitudes of the RPV contributions

In the RPV MSSM, in terms of the RPV superpotential [17], we can obtain the relative RPV effective Hamiltonian for $B\to D^{(*)}D_q^{(*)}$ decays as follows:

$$\begin{aligned}\mathcal{H}_{\rm eff}^{\rm RPV}=&\sum_n\frac{\lambda''_{ikn}\lambda''^{*}_{jln}}{2m_{\tilde d_n}^2}\eta^{-4/\beta_0}[-(\bar d_k\gamma^\mu P_Ru_j)_1(\bar u_i\gamma_\mu P_Rd_l)_1\\ &+(\bar d_k\gamma^\mu P_Ru_j)_8(\bar u_i\gamma_\mu P_Rd_l)_8]\\ &+\sum_i\frac{\lambda'_{ijk}\lambda'^{*}_{inl}}{m_{\tilde e_{iL}}^2}\eta^{-8/\beta_0}(\bar d_kP_Lu_j)_1(\bar u_nP_Rd_l)_1+{\rm H.c.},\end{aligned} \tag{18}$$

where $P_L=\frac{1-\gamma_5}{2}$, $P_R=\frac{1+\gamma_5}{2}$, $\eta=\frac{\alpha_s(m_{\tilde f})}{\alpha_s(m_b)}$, and $\beta_0=11-\frac{2}{3}n_f$. The subscripts 1 and 8 of the currents represent the currents in the color singlet and octet, respectively. The coefficients η^{-4/β_0} and η^{-8/β_0} are due to the running from the sfermion mass scale $m_{\tilde{f}}$ (assumed as 100 GeV) down to the m_b scale. Since it is usually assumed in phenomenology, for numerical display, that only one sfermion contributes at one time, we neglect the mixing between the operators when we use the renormalization group equation (RGE) to run $\mathcal{H}_{\rm eff}^{\rm RPV}$ down to the low scale.

The decay amplitudes of RPV contributions to $B \to D^{(*)} D_q^{(*)}$ are given by

$$\begin{aligned}\mathcal{M}^{\rm RPV}(B \to D^{(*)} D_q^{(*)}) = \Lambda''\left(-1 + \frac{1}{N_C}\right) &\times \langle D_q^{(*)}|\bar{q}\gamma_\mu(1+\gamma_5)c|0\rangle \\ &\times \langle D^{(*)}|\bar{c}\gamma_\mu(1+\gamma_5)b|B\rangle \\ &+ 2\Lambda'\langle D_q^{(*)}|\bar{q}(1-\gamma_5)c|0\rangle \\ &\times \langle D^{(*)}|\bar{c}(1+\gamma_5)b|B\rangle, \end{aligned} \tag{19}$$

$$= \begin{cases} [-\Lambda''(-1+\frac{1}{N_C}) + \xi\Lambda']A_{[BD,D_q]} & (DD_q) \\ [\Lambda''(-1+\frac{1}{N_C})]A_{[BD,D_q^*]} & (DD_q^*) \\ [\Lambda''(-1+\frac{1}{N_C}) - \xi\Lambda']A_{[BD^*,D_q]} & (D^*D_q) \\ [\Lambda''(-1+\frac{1}{N_C})]A'_{[BD^*,D_q^*]} & (D^*D_q^*), \end{cases} \tag{20}$$

where $\Lambda'' \equiv \eta^{-4/\beta_0}\frac{\lambda''^*_{232}\lambda''_{212}}{8m^2_{\tilde{s}}}$ $(\frac{\lambda''^*_{231}\lambda''_{221}}{8m^2_{\tilde{d}}})$ and $\Lambda' \equiv \eta^{-8/\beta_0}\sum_i \frac{\lambda'^*_{i23}\lambda'_{i21}}{8m^2_{\tilde{e}_{iL}}}$ $(\frac{\lambda'^*_{i23}\lambda'_{i22}}{8m^2_{\tilde{e}_{iL}}})$ for $q = d$ $(q = s)$. $A'_{[BD^*,D_q^*]}$ is defined by

$$\begin{aligned} A'_{[BD^*,D_q^*]} \equiv i f_{D_q^*} m_{D_q^*}\bigg[&(\varepsilon^*_{D^*}\cdot\varepsilon^*_{D_q^*})(m_B + m_{D^*})A_1(m^2_{D_q^*}) \\ &- (\varepsilon^*_{D^*}\cdot p_{D_q^*})(\varepsilon^*_{D_q^*}\cdot p_{D^*})\frac{2A_2(m^2_{D_q^*})}{m_B + m_{D^*}} \\ &- i\epsilon_{\mu\nu\alpha\beta}\varepsilon^{*\mu}_{D_q^*}\varepsilon^{*\nu}_{D^*}p^\alpha_{D_q^*}p^\beta_{D^*}\frac{2V(m^2_{D_q^*})}{m_B + m_{D^*}}\bigg]. \end{aligned} \tag{21}$$

C. Observables to be investigated

We can get the total decay amplitudes in the RPV MSSM as

$$\begin{aligned}\mathcal{M}(B \to D^{(*)}D_q^{(*)}) = \mathcal{M}^{\rm SM}(B \to D^{(*)}D_q^{(*)}) \\ + \mathcal{M}^{\rm RPV}(B \to D^{(*)}D_q^{(*)}). \end{aligned} \tag{22}$$

The branching ratio $\mathcal{B}$ reads

$$\mathcal{B}(B \to D^{(*)}D_q^{(*)}) = \frac{\tau_B|p_c|}{8\pi m_B^2}|\mathcal{M}(B \to D^{(*)}D_q^{(*)})|^2, \tag{23}$$

where τ_B is the B lifetime, and $|p_c|$ is the center-of-mass momentum in the center-of-mass frame of the B meson. In $B \to D^* D_q^*$ decays, the two vector mesons have the same helicity; therefore, three different polarization states, one longitudinal and two transverse, are possible. We define the corresponding amplitudes as $\mathcal{M}_{0,\pm}$ in the helicity basis and $\mathcal{M}_{L,\parallel,\perp}$ in the transversity basis, which are related by $\mathcal{M}_L = \mathcal{M}_0$ and $\mathcal{M}_{\parallel,\perp} = \frac{\mathcal{M}_+ \pm \mathcal{M}_-}{\sqrt{2}}$. Then we have

$$\begin{aligned}|\mathcal{M}(B \to D^*D_q^*)|^2 &= |\mathcal{M}_0|^2 + |\mathcal{M}_+|^2 + |\mathcal{M}_-|^2 \\ &= |\mathcal{M}_L|^2 + |\mathcal{M}_\parallel|^2 + |\mathcal{M}_\perp|^2. \end{aligned} \tag{24}$$

The longitudinal polarization fraction f_L and transverse polarization fraction $f_\perp$ are defined by

$$f_{L,\perp}(B \to D^*D_q^*) = \frac{\Gamma_{L,\perp}}{\Gamma} = \frac{|\mathcal{M}_{L,\perp}|^2}{|\mathcal{M}_L|^2 + |\mathcal{M}_\parallel|^2 + |\mathcal{M}_\perp|^2}. \tag{25}$$

In charged B meson decays, where mixing effects are absent, the only possible source of CPAs is

$$\mathcal{A}_{CP}^{k,\rm dir} = \frac{|\mathcal{M}_k(B^- \to \bar{f})/\mathcal{M}_k(B^+ \to f)|^2 - 1}{|\mathcal{M}_k(B^- \to \bar{f})/\mathcal{M}_k(B^+ \to f)|^2 + 1}, \tag{26}$$

and $k = L, \parallel, \perp$ for $B^- \to D^*D_q^*$ decays and $k = L$ for $B_u^- \to DD_q$, DD_q^*, D^*D_q decays. Then, for $B_u^- \to D^*D_q^*$ decays we have

$$\mathcal{A}_{CP}^{+,\rm dir}(B \to D^*D_q^*) = \frac{\mathcal{A}_{CP}^{\parallel,\rm dir}|\mathcal{M}_\parallel|^2 + \mathcal{A}_{CP}^{L,\rm dir}|\mathcal{M}_L|^2}{|\mathcal{M}_\parallel|^2 + |\mathcal{M}_L|^2}. \tag{27}$$

For CPAs of neutral B_q meson decays, there is an additional complication due to $B_q^0 - \bar{B}_q^0$ mixing. There are four cases that one encounters for neutral B_q decays, as discussed in Refs. [38–41].

(i) $B_q^0 \to f$, $\bar{B}_q^0 \to \bar{f}$, where f or $\bar{f}$ is not a common final state of B_q^0 and $\bar{B}_q^0$, for example, $B_q^0 \to D^+D_s^-$.

(ii) $B_q^0 \to (f = \bar{f}) \leftarrow \bar{B}_q^0$ with $f^{CP} = \pm f$, involving final states which are CP eigenstates, i.e., decays such as $B_d^0 \to D^+D^-$, $B_s^0 \to D_s^+D_s^-$.

(iii) $B_q^0 \to (f = \bar{f}) \leftarrow \bar{B}_q^0$ with $f^{CP} \neq \pm f$, involving final states which are not CP eigenstates. They include decays such as $B_q^0 \to (VV)^0$, since the VV states are not CP eigenstates.

(iv) $B_q^0 \to (f \& \bar{f}) \leftarrow \bar{B}_q^0$ with $f^{CP} \neq f$; i.e., both f and $\bar{f}$ are common final states of B_q^0 and $\bar{B}_q^0$, but they are not CP eigenstates. Decays $B_d^0(\bar{B}_d^0) \to D^{*-}D^+$, D^-D^{*+} and $B_s^0(\bar{B}_s^0) \to D_s^{*-}D_s^+$, $D_s^-D_s^{*+}$ belong to this case.

CPAs of neutral B decays in case (i) are similar to CPAs of the charged B decays, and there are only direct CPAs $\mathcal{A}_{CP}^{\rm dir}$ since no mixing is involved for these decays. For cases (ii) and (iii), their CPAs would involve $B_q^0 - \bar{B}_q^0$ mixing. The time-dependent asymmetries can be conveniently expressed as

$$\mathcal{A}_f^k(t) = \mathcal{S}_f^k \sin(\Delta m t) - \mathcal{C}_f^k \cos(\Delta m t), \tag{28}$$

$$\mathcal{S}_f^k \equiv \frac{2\,\mathrm{Im}(\lambda_k)}{1+|\lambda_k|^2}, \qquad \mathcal{C}_f^k \equiv \frac{1-|\lambda_k|^2}{1+|\lambda_k|^2}, \tag{29}$$

where $\lambda_k = \frac{q}{p}\frac{\mathcal{M}_k(\bar{B}^0 \to f)}{\mathcal{M}_k(B^0 \to f)}$. In addition, $\mathcal{S}_f^+$ and $\mathcal{C}_f^+$ can be obtained from a similar relation given in Eq. (27).

Case (iv) also involves mixing but requires additional formulas. Here one studies the four time-dependent decay widths for $B_q^0(t) \to f$, $\bar{B}_q^0(t) \to \bar{f}$, $B_q^0(t) \to \bar{f}$, and $\bar{B}_q^0(t) \to f$ [38–41]. These time-dependent widths can be expressed by four basic matrix elements [40],

$$\begin{aligned} g &= \langle f|\mathcal{H}_{\mathrm{eff}}|B_q^0\rangle, & h &= \langle f|\mathcal{H}_{\mathrm{eff}}|\bar{B}_q^0\rangle, \\ \bar{g} &= \langle \bar{f}|\mathcal{H}_{\mathrm{eff}}|\bar{B}_q^0\rangle, & \bar{h} &= \langle \bar{f}|\mathcal{H}_{\mathrm{eff}}|B_q^0\rangle, \end{aligned} \tag{30}$$

which determine the decay matrix elements of $B_q^0 \to f, \bar{f}$ and of $\bar{B}_q^0 \to f, \bar{f}$ at $t = 0$. We will study the following quantities:

$$\mathcal{S}_f^k = \frac{2\,\mathrm{Im}(\lambda_k')}{1+|\lambda_k'|^2}, \qquad \mathcal{C}_f^k = \frac{1-|\lambda_k'|^2}{1+|\lambda_k'|^2}, \tag{31}$$

$$\mathcal{S}_{\bar{f}}^k = \frac{2\,\mathrm{Im}(\lambda_k'')}{1+|\lambda_k''|^2}, \qquad \mathcal{C}_{\bar{f}}^k = \frac{1-|\lambda_k''|^2}{1+|\lambda_k''|^2}, \tag{32}$$

with $\lambda_k' = (q/p)(h/g)$ and $\lambda_k'' = (q/p)(\bar{g}/\bar{h})$. The signatures of CP violation are $\Gamma(\bar{B}_q^0(t) \to \bar{f}) \neq \Gamma(B_q^0(t) \to f)$ and $\Gamma(\bar{B}_q^0(t) \to f) \neq \Gamma(B_q^0(t) \to \bar{f})$, which means that $\mathcal{C}_f \neq -\mathcal{C}_{\bar{f}}$ and/or $\mathcal{S}_f \neq -\mathcal{S}_{\bar{f}}$.

D. Input parameters

Theoretical input parameters are collected in Table I. In our numerical results, we will use the input parameters which are varied randomly within the 1σ range.

We have several remarks on the input parameters:

(i) *CKM matrix elements*.—The weak phase γ is well constrained in the SM; however, with the presence of R-parity violation, this constraint may be relaxed. We will not take γ within the SM range, but vary it randomly in the range of 0 to π to obtain conservative limits on RPV couplings.

(ii) *Decay constants*.—The decay constants of D_q^* mesons have not been directly measured in experiments so far. In the heavy-quark limit ($m_c \to \infty$), spin symmetry predicts that $f_{D_q^*} = f_{D_q}$, and most theoretical predictions indicate that symmetry-breaking corrections enhance the ratio $f_{D_q^*}/f_{D_q}$ by 10%–20% [45,46]. Hence, we take $f_{D_q^*} = (1.1\text{–}1.2)f_{D_q}$ as our input values.

(iii) *Distribution amplitudes*.—The distribution amplitudes of $D_q^{(*)}$ mesons are less constrained, and we use the shape parameters $a_{D^{(*)}} = 0.7 \pm 0.2$ and $a_{D_s^{(*)}} = 0.3 \pm 0.2$.

(iv) *Form factors*.—For the form factors involving $B \to D^{(*)}$ transitions, we take expressions which include perturbative QCD corrections induced by hard gluon vertex corrections of $b \to c$ transitions and power corrections in orders of $1/m_{b,c}$ [37,47]. As for the Isgur-Wise function $\xi(\omega)$, we use the fit result $\xi(\omega) = 1 - 1.22(\omega - 1) + 0.85(\omega - 1)^2$ from Ref. [48].

(v) *Wilson coefficients*.—We obtain Wilson coefficients in terms of the expressions in [35].

(vi) *RPV couplings*.—When we study the RPV effects, we consider that only one RPV coupling product contributes at a time, neglecting the interferences between different RPV coupling products, but keeping their interferences with the SM amplitude. We assume the masses of the sfermions are 100 GeV. For other values of the sfermion masses, the bounds on the couplings in this paper can be easily obtained by scaling them by a factor $\tilde{f}^2 \equiv (\frac{m_{\tilde{f}}}{100\ \mathrm{GeV}})^2$.

III. NUMERICAL RESULTS AND DISCUSSIONS

In this section we summarize our numerical results and analysis in the exclusive color-allowed $b \to c\bar{c}q$ decays. First, we will show our estimates in the SM with full theoretical uncertainties of sensitive parameters. Then, we will investigate the RPV effects in the decays. We will constrain relevant RPV couplings only from very highly consistent experimental data and show the RPV MSSM predictions for the other observables, which have not been measured yet or have less consistency among different collaborations.

TABLE I. Summary of theoretical input parameters and $\pm 1\sigma$ error ranges for the sensitive parameters used in our numerical calculations.

$m_{B_u} = 5.279$ GeV, $m_{B_d} = 5.280$ GeV, $m_{B_s} = 5.366$ GeV, $M_{D^0} = 1.865$ GeV, $M_{D^+} = 1.870$ GeV, $M_{D_s^+} = 1.969$ GeV, $M_{D^{*0}} = 2.007$ GeV, $M_{D^{*+}} = 2.010$ GeV, $M_{D_s^{*+}} = 2.107$ GeV, $\bar{m}_b(\bar{m}_b) = (4.20 \pm 0.07)$ GeV, $\bar{m}_c(\bar{m}_c) = (1.25 \pm 0.09)$ GeV, $\bar{m}_s(2\ \mathrm{GeV}) = (0.095 \pm 0.025)$ GeV, $\bar{m}_u(2\ \mathrm{GeV}) = (0.0015\text{–}0.0030)$ GeV, $\bar{m}_d(2\ \mathrm{GeV}) = (0.003\text{–}0.007)$ GeV, $\tau_{B_u} = (1.638 \pm 0.011)$ ps, $\tau_{B_d} = (1.530 \pm 0.009)$ ps, $\tau_{B_s} = (1.425^{+0.041}_{-0.041})$ ps. [42]
$\lvert V_{ud}\rvert = 0.974\,30 \pm 0.000\,19$, $\lvert V_{us}\rvert = 0.225\,21^{+0.000\,83}_{-0.000\,82}$, $\lvert V_{ub}\rvert = 0.003\,44^{+0.000\,22}_{-0.000\,17}$, $\lvert V_{cd}\rvert = 0.225\,08^{+0.000\,84}_{-0.000\,82}$, $\lvert V_{cs}\rvert = 0.973\,50^{+0.000\,21}_{-0.000\,22}$, $\lvert V_{cb}\rvert = 0.040\,45^{+0.001\,06}_{-0.000\,78}$, $\lvert V_{td}\rvert = 0.008\,41^{+0.000\,35}_{-0.000\,92}$, $\lvert V_{ts}\rvert = 0.039\,72^{+0.001\,15}_{-0.000\,77}$, $\lvert V_{tb}\rvert = 0.999\,176^{+0.000\,031}_{-0.000\,044}$, $\alpha = (90.7^{+4.5}_{-2.9})^\circ$, $\beta = (21.7^{+1.0}_{-0.9})^\circ$, $\gamma = (67.6^{+2.8}_{-4.5})^\circ$. [43]
$f_D = (0.201 \pm 0.003 \pm 0.017)$ GeV, $f_{D_s} = (0.249 \pm 0.003 \pm 0.016)$ GeV. [44]

A. Exclusive color-allowed $b \to c\bar{c}d$ decays

The decays $\bar{B}_d^0 \to D^{(*)+}D^{(*)-}$, $B_u^- \to D^{(*)0}D^{(*)-}$, and $\bar{B}_s^0 \to D_s^{(*)+}D^{(*)-}$ are dominated by the color-allowed $b \to c\bar{c}d$ tree diagram, but involve small penguin pollution from the $b \to u\bar{u}d$ transition carrying a different weak phase. These decays involve the same set of RPV coupling constants, $\lambda''^{*}_{232}\lambda''_{212}$ and $\lambda'^{*}_{i23}\lambda'_{i21}$, at tree level due to squark and slepton exchanges, respectively. For $\bar{B}_d^0 \to D^{(*)+}D^{(*)-}$ and $B_u^- \to D^{(*)0}D^{(*)-}$ processes, a few observables have been measured by the *BABAR* and Belle collaborations. The latest experimental data and their weight averages are summarized in Table II. We can see that almost all physical quantities have been consistently measured between *BABAR* and Belle, and only $\mathcal{B}(\bar{B}_d^0 \to D^+D^-, D^{*\pm}D^{\mp})$, $\mathcal{C}(\bar{B}_d^0 \to D^+D^-)$, and $\mathcal{C}(B_d^0, \bar{B}_d^0 \to D^+D^{*-})$ have low consistency between *BABAR* and Belle.

Our SM estimates predicted within the theoretical uncertainties of input parameters are given in the second columns of Tables III and IV. Theoretical predictions for the branching ratios and the polarization fractions are given in Table III. CPA predictions are given in Table IV. All the branching ratios are above 10^{-4} order. The direct CPAs are expected to be quite small. All mixing-induced CPAs of $\bar{B}_d^0$ decays are very large (about -0.7). There is an obvious signature of the mixing-induced *CP* violations in $\bar{B}_s^0 \to D_s^{*+}D_s^-$, $D_s^+D_s^{*-}$ decays since $\mathcal{S}(B_s^0, \bar{B}_s^0 \to D_s^{*+}D_s^-) \neq -\mathcal{S}(B_s^0, \bar{B}_s^0 \to D_s^+D_s^{*-})$, which is consistent with the experimental measurements. In addition, for $\bar{B}_d^0 \to D^{*+}D^{*-}$, $B_u^- \to D^{*0}D^{*-}$, and $\bar{B}_s^0 \to D_s^{*+}D^{*-}$ decays, the longitudinal and transverse polarization fractions can be precisely predicted, and are about ~ 0.5 and ~ 0.1, respectively. Comparing present experimental data in Table II with the SM predictions in Tables III and IV, we can find that all measured quantities agree with the SM expectations within the error ranges, except $\mathcal{C}(B_d^0, \bar{B}_d^0 \to D^+D^-)$ from Belle.

We now turn to explore the RPV effects in $\bar{B}_d^0 \to D^{(*)+}D^{(*)-}$, $B_u^- \to D^{(*)0}D^{(*)-}$, and $\bar{B}_s^0 \to D_s^{(*)+}D^{(*)-}$ decays. The most conservative existing experimental bounds are used in our analysis. We choose the averaged data, which have highly consistent measurements between *BABAR* and Belle (defined as a scale factor $S \leq 1$), and vary randomly within 2σ ranges to constrain the RPV effects. The current experimental data and theoretical input parameters are not yet precise enough to set absolute bounds on the relative RPV couplings. We obtain the allowed scattering spaces of the RPV couplings $\lambda''^{*}_{232}\lambda''_{212}$ and $\lambda'^{*}_{i23}\lambda'_{i21}$ as displayed in Fig. 1. The parameter spaces that survived are not in conflict with the above-mentioned, highly consistent experimental data in $\bar{B}_d^0 \to D^{(*)+}D^{(*)-}$ and $B_u^- \to D^{(*)0}D^{(*)-}$ decays.

The squark exchange coupling $\lambda''^{*}_{232}\lambda''_{212}$ contributes to all 12 $\bar{B}_d^0 \to D^{(*)+}D^{(*)-}$, $B_u^- \to D^{(*)0}D^{(*)-}$, and $\bar{B}_s^0 \to D_s^{(*)+}D^{(*)-}$ decay modes. The allowed space of $\lambda''^{*}_{232}\lambda''_{212}$ is shown in the left plot of Fig. 1. Its magnitude $|\lambda''^{*}_{232}\lambda''_{212}|$ and its RPV weak phase ϕ_{RPV} have been constrained significantly. We obtain $|\lambda''^{*}_{232}\lambda''_{212}| \in [0.14, 1.62] \times 10^{-3}$

TABLE II. Experimental data for $\bar{B}_d^0 \to D^{(*)+}D^{(*)-}$ and $B_u^- \to D^{(*)0}D^{(*)-}$ decays from *BABAR* and Belle. The branching ratios ($\mathcal{B}$) are in units of 10^{-4}. The scale factor S is defined in the Introduction of Ref. [42], and $S > 1$ often indicates that the measurements are inconsistent.

Observable	*BABAR*	Belle	Average	S
$\mathcal{B}(\bar{B}_d^0 \to D^+D^-)$	$2.8 \pm 0.4 \pm 0.5$ [9]	$1.97 \pm 0.20 \pm 0.20$ [3]	2.1 ± 0.3	**1.2**
$\mathcal{B}(\bar{B}_d^0 \to D^{*\pm}D^{\mp})$	$5.7 \pm 0.7 \pm 0.7$ [9]	$11.7 \pm 2.6^{+2.2}_{-2.5}$ [26]	6.1 ± 1.5	**1.6**
$\mathcal{B}(\bar{B}_d^0 \to D^{*+}D^{*-})$	$8.1 \pm 0.6 \pm 1.0$ [9]	$8.1 \pm 0.8 \pm 1.1$ [7]	8.1 ± 0.9	≤ 1.0
$\mathcal{B}(B_u^- \to D^0D^-)$	$3.8 \pm 0.6 \pm 0.5$ [9]	$3.85 \pm 0.31 \pm 0.38$ [10]	3.8 ± 0.4	≤ 1.0
$\mathcal{B}(B_u^- \to D^{*0}D^-)$	$6.3 \pm 1.4 \pm 1.0$ [9]			
$\mathcal{B}(B_u^- \to D^0D^{*-})$	$3.6 \pm 0.5 \pm 0.4$ [9]	$4.57 \pm 0.71 \pm 0.56$ [11]	3.9 ± 0.5	≤ 1.0
$\mathcal{B}(B_u^- \to D^{*0}D^{*-})$	$8.1 \pm 1.2 \pm 1.2$ [9]			
$\mathcal{C}(\bar{B}_d^0 \to D^+D^-)$	$-0.07 \pm 0.23 \pm 0.03$ [4]	$-0.91 \pm 0.23 \pm 0.06$ [3]	-0.48 ± 0.42	**2.5**
$\mathcal{C}(B_d^0, \bar{B}_d^0 \to D^{*+}D^-)$	$0.08 \pm 0.17 \pm 0.04$ [4]	$-0.37 \pm 0.22 \pm 0.06$ [5]	-0.09 ± 0.22	**1.6**
$\mathcal{C}(B_d^0, \bar{B}_d^0 \to D^+D^{*-})$	$0.00 \pm 0.17 \pm 0.03$ [4]	$0.23 \pm 0.25 \pm 0.06$ [5]	0.07 ± 0.14	≤ 1.0
$\mathcal{C}^+(\bar{B}_d^0 \to D^{*+}D^{*-})$	$0.00 \pm 0.12 \pm 0.02$ [4]	$-0.15 \pm 0.13 \pm 0.04$ [8]	-0.07 ± 0.09	≤ 1.0
$\mathcal{A}_{CP}^{\mathrm{dir}}(B_u^- \to D^0D^-)$	$-0.13 \pm 0.14 \pm 0.02$ [9]	$0.00 \pm 0.08 \pm 0.02$ [10]	-0.03 ± 0.07	≤ 1.0
$\mathcal{A}_{CP}^{\mathrm{dir}}(B_u^- \to D^{*0}D^-)$	$0.13 \pm 0.18 \pm 0.04$ [9]			
$\mathcal{A}_{CP}^{\mathrm{dir}}(B_u^- \to D^0D^{*-})$	$-0.06 \pm 0.13 \pm 0.02$ [9]	$0.15 \pm 0.15 \pm 0.05$ [11]	0.03 ± 0.10	≤ 1.0
$\mathcal{A}_{CP}^{+,\mathrm{dir}}(B_u^- \to D^{*0}D^{*-})$	$-0.15 \pm 0.11 \pm 0.02$ [9]			
$\mathcal{S}(\bar{B}_d^0 \to D^+D^-)$	$-0.63 \pm 0.36 \pm 0.05$ [4]	$-1.13 \pm 0.37 \pm 0.09$ [3]	-0.87 ± 0.26	≤ 1.0
$\mathcal{S}(B_d^0, \bar{B}_d^0 \to D^{*+}D^-)$	$-0.62 \pm 0.21 \pm 0.03$ [4]	$-0.55 \pm 0.39 \pm 0.12$ [5]	-0.61 ± 0.19	≤ 1.0
$\mathcal{S}(B_d^0, \bar{B}_d^0 \to D^+D^{*-})$	$-0.73 \pm 0.23 \pm 0.05$ [4]	$-0.96 \pm 0.43 \pm 0.12$ [5]	-0.78 ± 0.21	≤ 1.0
$\mathcal{S}^+(\bar{B}_d^0 \to D^{*+}D^{*-})$	$-0.76 \pm 0.16 \pm 0.04$ [4]	$-0.96 \pm 0.25^{+0.12}_{-0.16}$ [8]	-0.81 ± 0.14	≤ 1.0
$f_\perp(\bar{B}_d^0 \to D^{*+}D^{*-})$	$0.158 \pm 0.028 \pm 0.006$ [4]	$0.125 \pm 0.043 \pm 0.023$ [8]	0.150 ± 0.025	≤ 1.0
$f_L(\bar{B}_d^0 \to D^{*+}D^{*-})$		$0.57 \pm 0.08 \pm 0.02$ [7]		

TABLE III. Theoretical predictions for CP-averaged branching ratios (in units of 10^{-4}) and ratios of polarization (in units of 10^{-2}) in exclusive color-allowed $b \to c\bar{c}d$ decays. The second column gives the SM predictions with the theoretical uncertainties of the input parameters. The last two columns are the RPV MSSM predictions with different RPV couplings, considering the input parameter uncertainties and experimental errors.

Observable	SM	MSSM w/$\lambda''^{*}_{232}\lambda''_{212}$	MSSM w/$\lambda'^{*}_{i23}\lambda'_{i21}$
$\mathcal{B}(\bar{B}^0_d \to D^+D^-)$	[2.35, 4.15]	[2.77, 3.80]	[2.77, 4.39]
$\mathcal{B}(\bar{B}^0_d \to D^{*+}D^-)$	[2.27, 3.96]	[2.87, 4.22]	[2.30, 4.59]
$\mathcal{B}(\bar{B}^0_d \to D^+D^{*-})$	[2.56, 5.04]	[3.31, 4.65]	
$\mathcal{B}(\bar{B}^0_d \to D^{*\pm}D^{\mp})$	[4.84, 8.95]	[6.18, 8.70]	[5.21, 8.84]
$\mathcal{B}(\bar{B}^0_d \to D^{*+}D^{*-})$	[6.21, 12.22]	[7.05, 8.90]	
$\mathcal{B}(B^-_u \to D^0D^-)$	[2.53, 4.43]	[3.00, 4.04]	[3.00, 4.68]
$\mathcal{B}(B^-_u \to D^{*0}D^-)$	[2.42, 4.27]	[3.07, 4.53]	[2.25, 4.75]
$\mathcal{B}(B^-_u \to D^0D^{*-})$	[2.73, 5.42]	[3.55, 4.96]	
$\mathcal{B}(B^-_u \to D^{*0}D^{*-})$	[6.61, 13.10]	[7.54, 10.67]	
$\mathcal{B}(\bar{B}^0_s \to D^+_sD^-)$	[2.33, 4.20]	[2.76, 3.81]	[2.77, 4.48]
$\mathcal{B}(\bar{B}^0_s \to D^{*+}_sD^-)$	[2.24, 4.00]	[2.81, 4.25]	[2.08, 4.42]
$\mathcal{B}(\bar{B}^0_s \to D^+_sD^{*-})$	[2.54, 5.03]	[3.27, 4.69]	
$\mathcal{B}(\bar{B}^0_s \to D^{*+}_sD^{*-})$	[6.15, 12.10]	[6.92, 10.04]	
$f_L(\bar{B}^0_d \to D^{*+}D^{*-})$	[52.40, 52.97]	[50.35, 52.53]	
$f_L(B^-_u \to D^{*0}D^{*-})$	[52.43, 53.02]	[50.37, 52.56]	
$f_L(\bar{B}^0_s \to D^{*+}_sD^{*-})$	[52.56, 53.16]	[50.60, 52.70]	
$f_\perp(\bar{B}^0_d \to D^{*+}D^{*-})$	[8.82, 9.51]	[10.00, 12.94]	
$f_\perp(B^-_u \to D^{*0}D^{*-})$	[8.84, 9.53]	[10.03, 12.97]	
$f_\perp(\bar{B}^0_s \to D^{*+}_sD^{*-})$	[8.35, 9.05]	[9.50, 12.34]	

and $\phi_{\rm RPV} \in [-75°, 84°]$. The right plot of Fig. 1 displays the allowed space of the RPV couplings $\lambda'^{*}_{i23}\lambda'_{i21}$ due to slepton exchanges, which contributes only to six decay modes, $\bar{B}^0_d \to D^{(*)+}D^-$, $B^-_u \to D^{(*)0}D^-$, and $\bar{B}^0_s \to D^{(*)+}_sD^-$. The magnitudes $|\lambda'^{*}_{i23}\lambda'_{i21}|$ have been limited within $|\lambda'^{*}_{i23}\lambda'_{i21}| \leq 1.28 \times 10^{-3}$, and the corresponding RPV weak phase $\phi_{\rm RPV}$ for the range $|\lambda'^{*}_{i23}\lambda'_{i21}| \leq 0.4 \times 10^{-3}$ is not constrained so much; however, the RPV weak phase for $|\lambda'^{*}_{i23}\lambda'_{i21}| \in [0.4, 1.3] \times 10^{-3}$ is very narrow.

Using the constrained parameter spaces shown in Fig. 1, one may predict the RPV effects on the other quantities which have not been measured yet or have less consistent measurements between *BABAR* and Belle. With the expressions for $\mathcal{B}$, $\mathcal{C}$, $\mathcal{S}$, $\mathcal{A}^{\rm dir}_{CP}$, f_L, and $f_\perp$ at hand, we perform a scan on the input parameters and the constrained RPV couplings. Then we obtain the RPV MSSM predictions with different RPV coupling, whose numerical results are summarized in the last two columns of Tables III and IV.

TABLE IV. Theoretical predictions for CPAs (in units of 10^{-2}) in exclusive color-allowed $b \to c\bar{c}d$ decays.

Observable	SM	MSSM w/$\lambda''^{*}_{232}\lambda''_{212}$	MSSM w/$\lambda'^{*}_{i23}\lambda'_{i21}$
$\mathcal{S}(B^0_d, \bar{B}^0_d \to D^+D^-)$	[− 78.00, −71.67]	[− 97.52, −52.66]	[− 99.83, −35.16]
$\mathcal{S}(B^0_d, \bar{B}^0_d \to D^{*+}D^-)$	[− 70.40, −64.55]	[− 81.77, −32.17]	[− 98.01, −55.02]
$\mathcal{S}(B^0_d, \bar{B}^0_d \to D^+D^{*-})$	[− 72.17, −66.83]	[− 83.29, −36.15]	[− 98.30, −57.69]
$\mathcal{S}^+(B^0_d, \bar{B}^0_d \to D^{*+}D^{*-})$	[− 72.73, −67.77]	[− 95.18, −53.01]	
$\mathcal{C}(B^0_d, \bar{B}^0_d \to D^+D^-)$	[− 6.03, −3.87]	[− 7.61, 0.92]	[− 11.05, 2.59]
$\mathcal{C}(B^0_d, \bar{B}^0_d \to D^{*+}D^-)$	[3.36, 13.83]	[1.38, 14.75]	[− 13.35, 21.30]
$\mathcal{C}(B^0_d, \bar{B}^0_d \to D^+D^{*-})$	[− 14.44, −3.53	[− 14.83, −1.45]	[− 21.00, 13.28]
$\mathcal{C}^+(B^0_d, \bar{B}^0_d \to D^{*+}D^{*-})$	[− 1.35, −1.03]	[− 1.83, 0.20]	
$\mathcal{A}^{\rm dir}_{CP}(B^-_u \to D^0D^-)$	[3.87, 6.03]	[− 0.92, 7.61]	[− 2.59, 11.05]
$\mathcal{A}^{\rm dir}_{CP}(B^-_u \to D^{*0}D^-)$	[− 1.15, −0.45	[− 1.10, 0.29]	[− 1.99, 0.23]
$\mathcal{A}^{\rm dir}_{CP}(B^-_u \to D^0D^{*-})$	[1.03, 1.35]	[− 0.40, 1.42]	
$\mathcal{A}^{+,dir}_{CP}(B^-_u \to D^{*0}D^{*-})$	[1.03, 1.35]	[− 0.20, 1.83]	
$\mathcal{A}^{\rm dir}_{CP}(\bar{B}^0_s \to D^+_sD^-)$	[3.87, 6.03]	[− 0.92, 7.61]	[− 2.59, 11.05]
$\mathcal{A}^{\rm dir}_{CP}(\bar{B}^0_s \to D^{*+}_sD^-)$	[− 1.15, −0.45]	[− 1.10, 0.29]	[− 1.99, 0.23]
$\mathcal{A}^{\rm dir}_{CP}(\bar{B}^0_s \to D^+_sD^{*-})$	[1.03, 1.35]	[− 0.40, 1.42]	
$\mathcal{A}^{+,\rm dir}_{CP}(\bar{B}^0_s \to D^{*+}_sD^{*-})$	[1.03, 1.35]	[− 0.20, 1.83]	

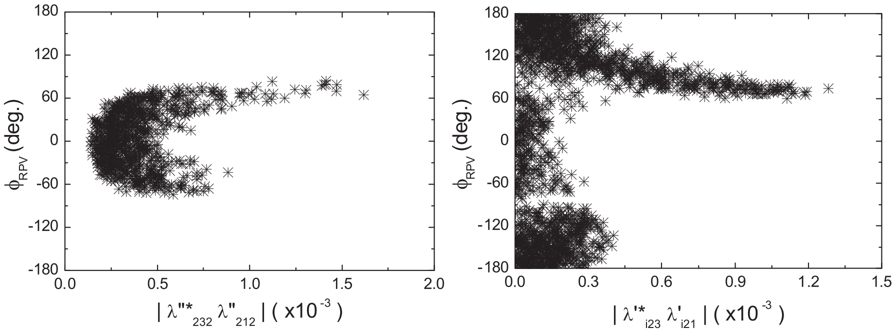

FIG. 1. Allowed parameter spaces for relevant RPV couplings constrained by $\bar{B}^0_d \to D^{(*)+}D^{(*)-}$ and $B^-_u \to D^{(*)0}D^{(*)-}$, where $\phi_{\rm RPV}$ denotes the RPV weak phase.

The contributions of $\lambda''^{*}_{232}\lambda''_{212}$ due to squark exchange are summarized in the third columns of Tables III and IV. In Table III, comparing with the SM predictions, we find that the $\lambda''^{*}_{232}\lambda''_{212}$ coupling could not affect all branching ratios much. Three $f_L(B \to D^*D^*)$ and three $f_\perp(B \to D^*D^*)$ are slightly decreased and increased by the $\lambda''^{*}_{232}\lambda''_{212}$ coupling, respectively, and their allowed ranges are scarcely magnified by this coupling. As given in Table IV, the $\lambda''^{*}_{232}\lambda''_{212}$ contributions could greatly enlarge the ranges of four $\mathcal{S}(B^0_d, \bar{B}^0_d \to D^{(*)+}D^{(*)-})$. The effects of the $\lambda''^{*}_{232}\lambda''_{212}$ coupling could extend the allowed regions of four $\mathcal{C}(B^0_d, \bar{B}^0_d \to D^{(*)+}D^{(*)-})$ and eight $\mathcal{A}^{\rm dir}_{CP}(B^-_u \to D^{(*)0}D^{(*)-}, \bar{B}^0_s \to D^{(*)+}_s D^{(*)-})$ a little bit, too. But this squark exchange coupling cannot explain the large $\mathcal{C}(B^0_d, \bar{B}^0_d \to D^+D^-)$ from Belle. The predictions including slepton exchange couplings $\lambda'^{*}_{i23}\lambda'_{i21}$ are listed in the last columns of Tables III and IV. The $\lambda'^{*}_{i23}\lambda'_{i21}$ couplings do not give very big effects on the relevant branching ratios, but could significantly magnify the ranges of $\mathcal{S}(B^0_d, \bar{B}^0_d \to D^{(*)+}D^-)$ from their SM predictions as well as extend the ranges of $\mathcal{C}(B^0_d, \bar{B}^0_d \to D^{(*)+}D^-)$ and $\mathcal{A}^{\rm dir}_{CP}(B^-_u \to D^{(*)0}D^-, \bar{B}^0_s \to D^{(*)+}_s D^-)$. The lower limits of $\mathcal{C}(B^0_d, \bar{B}^0_d \to D^{(*)+}D^-)$ could be reduced by these slepton exchange couplings, too, but slepton exchange coupling effects are still not large enough to explain the large $\mathcal{C}(B^0_d, \bar{B}^0_d \to D^+D^-)$ from Belle.

It is worth noting that our investigation of the color-allowed $b \to c\bar{c}d$ decays was motivated by the large direct CPA of $\bar{B}^0_d \to D^+D^-$ reported by Belle [3], which has not been confirmed by *BABAR* and contradicted the SM prediction. Relative RPV couplings, constrained by all consistent measurements in $\bar{B}^0_d \to D^{(*)+}D^{(*)-}$ and $B^-_u \to D^{(*)0}D^{(*)-}$ systems, could slightly enlarge the range of $\mathcal{C}(B^0_d, \bar{B}^0_d \to D^+D^-)$. Our RPV MSSM prediction for this observable is coincident with the *BABAR* measurement, but still cannot explain the Belle measurement. The unparticle interaction has positive effects on $\mathcal{C}(B^0_d, \bar{B}^0_d \to D^+D^-)$, as obtained in Ref. [12], in which the author used only experimental constraints of $\mathcal{B}(\bar{B}^0_d \to D^+D^-)$. Note also that very large values of $\mathcal{C}(B^0_d, \bar{B}^0_d \to D^+D^-)$ could be obtained by unparticle interaction, but with the sign opposite to the Belle measurement.

For each RPV coupling product, we can present correlations of physical quantities within the constrained parameter spaces displayed in Fig. 1 by the three-dimensional scatter plots. RPV coupling contributions to $\bar{B}^0_d \to D^{(*)+}D^{(*)-}$, $B^-_u \to D^{(*)0}D^{(*)-}$, and $\bar{B}^0_s \to D^{(*)+}_s D^{(*)-}$ decays are very similar to each other. So we will take as an example a few observables of the $\bar{B}^0_d \to D^{(*)+}D^{(*)-}$ decays to illustrate RPV coupling effects. Effects of RPV couplings $\lambda''^{*}_{232}\lambda''_{212}$ and $\lambda'^{*}_{i23}\lambda'_{i21}$ on observables of $\bar{B}^0_d \to D^{(*)+}D^{(*)-}$ decays are shown in Figs. 2 and 3, respectively.

In Fig. 2, we plot $\mathcal{B}$, f_L, $\mathcal{C}$, and $\mathcal{S}$ as functions of $\lambda''^{*}_{232}\lambda''_{212}$. The three-dimensional scatter plot in Fig. 2(a) shows $\mathcal{B}(\bar{B}^0_d \to D^+D^-)$ correlated with $|\lambda''^{*}_{232}\lambda''_{212}|$ and its phase $\phi_{\rm RPV}$. We also give projections to three perpendicular planes, where the $|\lambda''^{*}_{232}\lambda''_{212}|$-$\phi_{\rm RPV}$ plane displays the constrained regions of $\lambda''^{*}_{232}\lambda''_{212}$, as shown in the left plot of Fig. 1. It is shown that $\mathcal{B}(\bar{B}^0_d \to D^+D^-)$ only decreases a little with $|\lambda''^{*}_{232}\lambda''_{212}|$ on the $\mathcal{B}$-$|\lambda''^{*}_{232}\lambda''_{212}|$ plane. From the $\mathcal{B}$-$\phi_{\rm RPV}$ plane, we see that $\mathcal{B}(\bar{B}^0_d \to D^+D^-)$ is not sensitive to $\phi_{\rm RPV}$. All other branching ratios have similar trends to the $\lambda''^{*}_{232}\lambda''_{212}$ coupling. From Figs. 2(b)–2(d), we can see that $f_L(\bar{B}^0_d \to D^{*+}D^{*-})$ and $\mathcal{C}(B^0_d, \bar{B}^0_d \to D^+D^-, D^{*+}D^-)$ are not very sensitive to $|\lambda''^{*}_{232}\lambda''_{212}|$ and $\phi_{\rm RPV}$. Contributions from the RPV coupling $\lambda''^{*}_{232}\lambda''_{212}$ to $\mathcal{S}(B^0_d, \bar{B}^0_d \to D^+D^-, D^{*+}D^{*-})$ are also very similar to each other. So we take an example for $\mathcal{S}(B^0_d, \bar{B}^0_d \to D^+D^-)$, shown in Fig. 2(e), to illustrate the RPV coupling effects. $\mathcal{S}(B^0_d, \bar{B}^0_d \to D^+D^-)$ is decreasing (increasing) with $|\lambda''^{*}_{232}\lambda''_{212}|$ when $\phi_{\rm RPV} > 0$ ($\phi_{\rm RPV} < 0$), and it is decreasing with $\phi_{\rm RPV}$. $\mathcal{S}(B^0_d, \bar{B}^0_d \to D^{*+}D^-, D^+D^{*-})$ decays have totally different trends than $\mathcal{S}(B^0_d, \bar{B}^0_d \to D^+D^-)$ with $|\lambda''^{*}_{232}\lambda''_{212}|$ and $\phi_{\rm RPV}$, and we show only the squark exchange effects on $\mathcal{S}(B^0_d, \bar{B}^0_d \to D^{*+}D^-)$ in Fig. 2(f).

Figure 3 gives the effects of the slepton exchange couplings $\lambda'^{*}_{i23}\lambda'_{i21}$ in $\bar{B}^0_d \to D^{(*)+}D^-$ decays. As displayed in Fig. 3(a), $\mathcal{B}(\bar{B}^0_d \to D^+D^-)$ is not very sensitive to $|\lambda'^{*}_{i23}\lambda'_{i21}|$ and has only small allowed values when $|\phi_{\rm RPV}|$ is small. Figure 3(b) shows that $\mathcal{B}(\bar{B}^0_d \to D^{*+}D^-)$ is de-

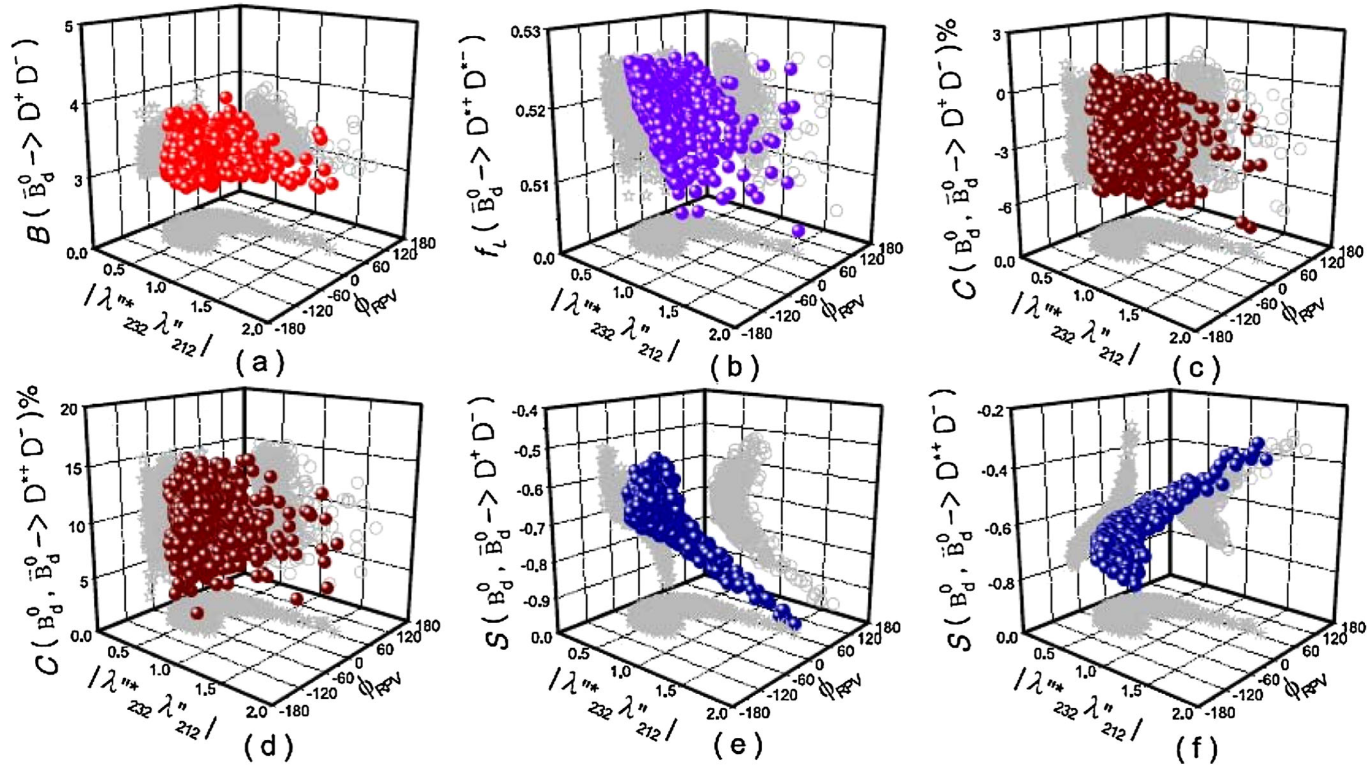

FIG. 2 (color online). Effects of the RPV coupling $\lambda''^{*}_{232}\lambda''_{212}$ on $\bar{B}^0_d \to D^{(*)+}D^{(*)-}$ decays, where $|\lambda''^{*}_{232}\lambda''_{212}|$ is in units of 10^{-3} and $\mathcal{B}$ in units of 10^{-4}.

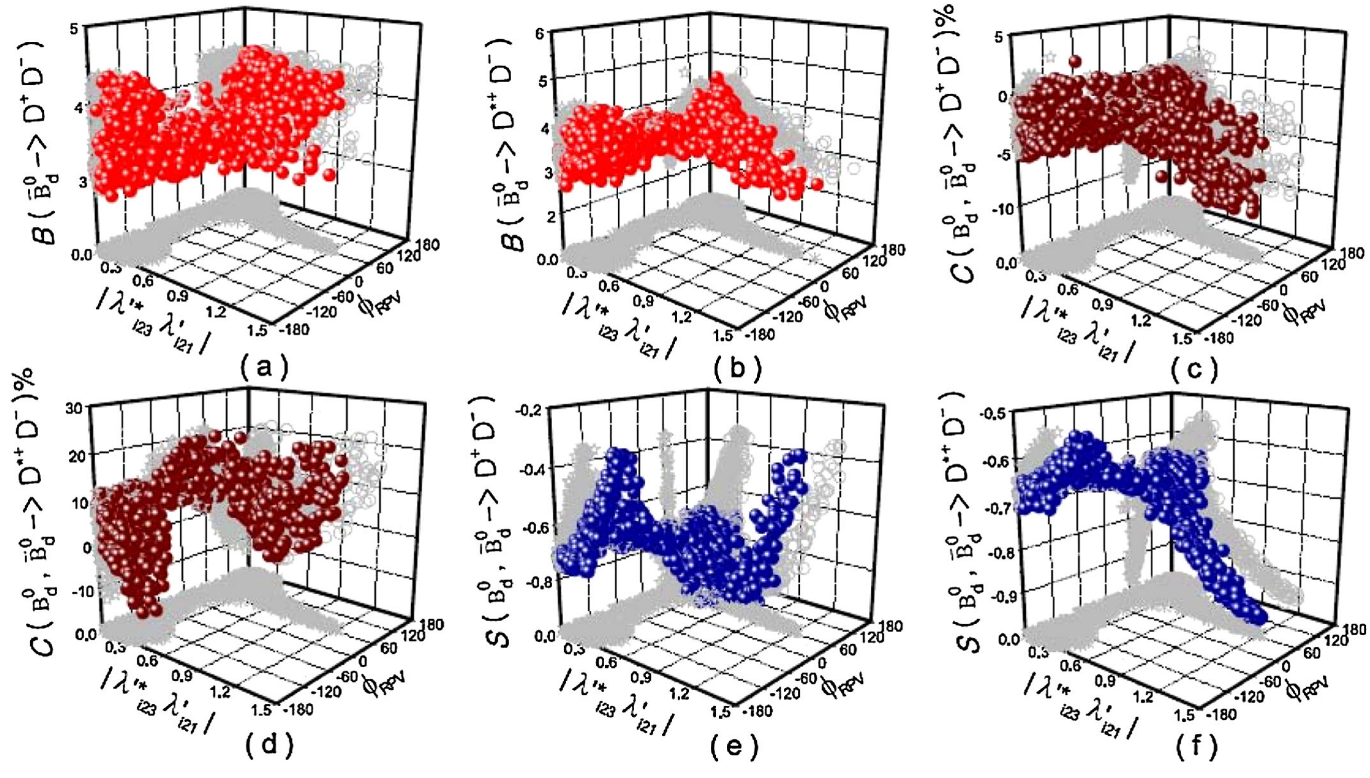

FIG. 3 (color online). Effects of the RPV coupling $\lambda'^{*}_{i23}\lambda'_{i21}$ on $\bar{B}^0_d \to D^{(*)+}D^{-}$ decays, where $|\lambda'^{*}_{i23}\lambda'_{i21}|$ is in units of 10^{-3} and $\mathcal{B}$ in units of 10^{-4}.

creasing with $|\lambda'^*_{i23}\lambda'_{i21}|$ and is weakly sensitive to $|\phi_{\rm RPV}|$. Figure 2(c) exhibits the slepton exchange coupling effects on $\mathcal{C}(B^0_d, \bar{B}^0_d \to D^+D^-)$, which is decreasing with $|\lambda'^*_{i23}\lambda'_{i21}|$ and has little sensitivity to $\phi_{\rm RPV}$. Slepton exchange couplings have great effects on $\mathcal{C}(B^0_d, \bar{B}^0_d \to D^{*+}D^-, D^+D^{*-})$ and $\mathcal{S}(B^0_d, \bar{B}^0_d \to D^+D^-, D^{*+}D^-, D^+D^{*-})$, and they have quite complex variational trends to $|\lambda'^*_{i23}\lambda'_{i21}|$ and $|\phi_{\rm RPV}|$. The effects of $\lambda'^*_{i23}\lambda'_{i21}$ couplings on $\mathcal{C}(B^0_d, \bar{B}^0_d \to D^{*+}D^-)$ and $\mathcal{S}(B^0_d, \bar{B}^0_d \to D^+D^-, D^{*+}D^-)$ are shown in Figs. 3(d)–3(f). $\mathcal{C}(B^0_d, \bar{B}^0_d \to D^+D^{*-})$ has entirely different trends from $\mathcal{C}(B^0_d, \bar{B}^0_d \to D^{*+}D^-)$. $\mathcal{S}(B^0_d, \bar{B}^0_d \to D^+D^{*-})$ has a similar trend as $\mathcal{S}(B^0_d, \bar{B}^0_d \to D^{*+}D^-)$.

B. Exclusive color-allowed $b \to c\bar{c}s$ decays

Exclusive color-allowed $b \to c\bar{c}s$ tree decays include $\bar{B}^0_d \to D^{(*)+}D^{(*)-}_s$, $B^-_u \to D^{(*)0}D^{(*)-}_s$, and $\bar{B}^0_s \to D^{(*)+}_s D^{(*)-}_s$ decay modes. Almost all branching ratios and one longitudinal polarization have been measured by the Belle [49], *BABAR* [27–29], CLEO [30–33], and ARGUS [34] collaborations. Their averaged values from the Particle Data Group [42] are listed as follows:

$$\begin{aligned}
&\mathcal{B}(\bar{B}^0_d \to D^+D^-_s) = (7.4 \pm 0.7) \times 10^{-3}, \qquad \mathcal{B}(\bar{B}^0_d \to D^{*+}D^-_s) = (8.3 \pm 1.1) \times 10^{-3},\\
&\mathcal{B}(\bar{B}^0_d \to D^+D^{*-}_s) = (7.6 \pm 1.6) \times 10^{-3}, \qquad \mathcal{B}(\bar{B}^0_d \to D^{*+}D^{*-}_s) = (17.9 \pm 1.4) \times 10^{-3},\\
&\mathcal{B}(B^-_u \to D^0D^-_s) = (10.3 \pm 1.7) \times 10^{-3}, \qquad \mathcal{B}(B^-_u \to D^{*0}D^-_s) = (8.4 \pm 1.7) \times 10^{-3},\\
&\mathcal{B}(B^-_u \to D^0D^{*-}_s) = (7.8 \pm 1.6) \times 10^{-3}, \qquad \mathcal{B}(B^-_u \to D^{*0}D^{*-}_s) = (17.5 \pm 2.3) \times 10^{-3},\\
&\mathcal{B}(\bar{B}^0_s \to D^+_sD^-_s) = (11 \pm 4) \times 10^{-3}, \qquad \mathcal{B}(\bar{B}^0_s \to D^+_sD^{*-}_s) < 121 \times 10^{-3},\\
&\mathcal{B}(\bar{B}^0_s \to D^{*+}_sD^{*-}_s) < 257 \times 10^{-3}, \qquad f_L(\bar{B}^0_d \to D^{*+}D^{*-}_s) = 0.52 \pm 0.05.
\end{aligned} \tag{33}$$

The SM predictions, in which the full theoretical uncertainties of input parameters are considered, are given in the second columns of Tables V and VI. Theoretical predictions for the branching ratios and the polarization fractions are given in Table V. Predicted CPAs are also given in Table VI. Compared with the experimental data, only the SM predictions of $\mathcal{B}(\bar{B}^0_d \to D^{*+}D^{*-}_s, B^-_u \to D^{*0}D^{*-}_s)$ are slightly larger than the corresponding experimental data given in Eq. (33), and all the other branching ratios are consistent with the data within the 1σ error level. For the color-allowed $b \to c\bar{c}s$ decays the penguin effects are doubly Cabibbo suppressed and, therefore, play a significantly less pronounced role in CPAs. These CPAs have not been measured yet. We find that all CPAs are expected to be very small (about 10^{-3} or 10^{-4} order) in the SM except $\mathcal{S}(B^0_s, \bar{B}^0_s \to D^{*+}_sD^{*-}_s)$ and $\mathcal{C}(B^0_s, \bar{B}^0_s \to D^{*+}_sD^-_s, D^+_sD^{*-}_s)$. There is no obvious signature of *CP* violation in $B_s \to D^{*\pm}_sD^{\mp}_s$ decays since $\mathcal{C}(B^0_s, \bar{B}^0_s \to D^{*+}_sD^-_s) \approx -\mathcal{C}(B^0_s, \bar{B}^0_s \to D^+_sD^{*-}_s)$ and $\mathcal{S}(B^0_s, \bar{B}^0_s \to D^{*+}_sD^-_s) \approx -\mathcal{S}(B^0_s, \bar{B}^0_s \to D^+_sD^{*-}_s)$.

TABLE V. Theoretical predictions for *CP*-averaged $\mathcal{B}$ (in units of 10^{-4}) and polarization fractions (in units of 10^{-2}) of exclusive color-allowed $b \to c\bar{c}s$ decays in the SM and the RPV MSSM.

Observable	SM	MSSM w/$\lambda''^*_{231}\lambda''_{221}$	MSSM w/$\lambda'^*_{i23}\lambda'_{i22}$
$\mathcal{B}(\bar{B}^0_d \to D^+D^-_s)$	[6.70, 10.65]	[6.38, 7.59]	[6.42, 8.80]
$\mathcal{B}(\bar{B}^0_d \to D^{*+}D^-_s)$	[6.70, 10.45]	[6.47, 9.49]	[6.16, 9.30]
$\mathcal{B}(\bar{B}^0_d \to D^+D^{*-}_s)$	[7.32, 13.22]	[6.90, 10.29]	
$\mathcal{B}(\bar{B}^0_d \to D^{*+}D^{*-}_s)$	[19.27, 34.42]	[18.59, 20.70]	
$\mathcal{B}(B^-_u \to D^0D^-_s)$	[7.21, 11.43]	[6.90, 8.12]	[6.90, 9.49]
$\mathcal{B}(B^-_u \to D^{*0}D^-_s)$	[7.17, 11.24]	[6.95, 10.17]	[6.64, 9.96]
$\mathcal{B}(B^-_u \to D^0D^{*-}_s)$	[7.89, 14.27]	[7.43, 11.00]	
$\mathcal{B}(B^-_u \to D^{*0}D^{*-}_s)$	[20.57, 37.06]	[19.99, 22.10]	
$\mathcal{B}(\bar{B}^0_s \to D^+_sD^-_s)$	[6.55, 10.72]	[6.36, 7.71]	[6.23, 9.05]
$\mathcal{B}(\bar{B}^0_s \to D^{*+}_sD^-_s)$	[6.46, 10.44]	[6.51, 9.46]	[6.02, 9.26]
$\mathcal{B}(\bar{B}^0_s \to D^+_sD^{*-}_s)$	[7.08, 12.97]	[7.00, 10.40]	
$\mathcal{B}(\bar{B}^0_s \to D^{*+}_sD^{*-}_s)$	[18.64, 33.83]	[18.48, 20.93]	
$f_L(\bar{B}^0_d \to D^{*+}D^{*-}_s)$	[50.25, 50.91]	[48.46, 51.13]	
$f_L(B^-_u \to D^{*0}D^{*-}_s)$	[50.28, 50.94]	[48.49, 51.16]	
$f_L(\bar{B}^0_s \to D^{*+}_sD^{*-}_s)$	[50.40, 51.10]	[48.71, 51.30]	
$f_\perp(\bar{B}^0_d \to D^{*+}D^{*-}_s)$	[8.85, 9.55]	[8.15, 12.85]	
$f_\perp(B^-_u \to D^{*0}D^{*-}_s)$	[8.87, 9.57]	[8.17, 12.88]	
$f_\perp(\bar{B}^0_s \to D^{*+}_sD^{*-}_s)$	[8.38, 9.07]	[7.71, 12.23]	

TABLE VI. Theoretical predictions for CPAs (in units of 10^{-2}) of exclusive color-allowed $b \to c\bar{c}s$ decays in the SM and the RPV MSSM.

Observable	SM	MSSM w/$\lambda''^{*}_{231}\lambda''_{221}$	MSSM w/$\lambda'^{*}_{i23}\lambda'_{i22}$
$\mathcal{A}^{\rm dir}_{CP}(\bar{B}^0_d \to D^+ D^-_s)$	$[-0.34, -0.22]$	$[-3.06, 2.58]$	$[-8.42, 7.94]$
$\mathcal{A}^{\rm dir}_{CP}(\bar{B}^0_d \to D^{*+} D^-_s)$	$[0.03, 0.06]$	$-0.32, 0.36]$	$-0.98, 1.07]$
$\mathcal{A}^{\rm dir}_{CP}(\bar{B}^0_d \to D^+ D^{*-}_s)$	$[-0.07, -0.06]$	$-0.51, 0.44]$	
$\mathcal{A}^{+,\rm dir}_{CP}(\bar{B}^0_d \to D^{*+} D^{*-}_s)$	$[-0.07, -0.06]$	$[-0.69, 0.56]$	
$\mathcal{A}^{\rm dir}_{CP}(B^-_u \to D^0 D^-_s)$	$[-0.34, -0.22]$	$[-3.06, 2.58]$	$[-8.42, 7.94]$
$\mathcal{A}^{\rm dir}_{CP}(B^-_u \to D^{*0} D^-_s)$	$[0.03, 0.06]$	$[-0.32, 0.36]$	$[-0.98, 1.07]$
$\mathcal{A}^{\rm dir}_{CP}(B^-_u \to D^0 D^{*-}_s)$	$[-0.07, -0.06]$	$[-0.51, 0.58]$	
$\mathcal{A}^{+,\rm dir}_{CP}(B^-_u \to D^{*0} D^{*-}_s)$	$[-0.07, -0.06]$	$[-0.69, 0.56]$	
$\mathcal{S}(B^0_s, \bar{B}^0_s \to D^+_s D^-_s)$	$[0.40, 0.61]$	$[-59.67, 61.80]$	$[-99.84, 99.79]$
$\mathcal{S}(B^0_s, \bar{B}^0_s \to D^{*+}_s D^-_s)$	$[1.33, 2.16]$	$[-46.48, 47.65]$	$[-56.04, 59.14]$
$\mathcal{S}(B^0_s, \bar{B}^0_s \to D^+_s D^{*-}_s)$	$[-2.20, -1.31]$	$[-49.26, 45.22]$	$[-58.96, 56.60]$
$\mathcal{S}^+(B^0_s, \bar{B}^0_s \to D^{*+}_s D^{*-}_s)$	$[-31.81, -29.15]$	$[-54.41, 55.49]$	
$\mathcal{C}(B^0_s, \bar{B}^0_s \to D^+_s D^-_s)$	$[0.22, 0.34]$	$[-2.58, 3.06]$	$[-7.94, 8.42]$
$\mathcal{C}(B^0_s, \bar{B}^0_s \to D^{*+}_s D^-_s)$	$[2.77, 13.39]$	$[3.15, 10.13]$	$[0.79, 28.22]$
$\mathcal{C}(B^0_s, \bar{B}^0_s \to D^+_s D^{*-}_s)$	$[-13.36, -2.76]$	$[-10.08, -3.14]$	$[-29.14, -0.54]$
$\mathcal{C}^+(B^0_s, \bar{B}^0_s \to D^{*+}_s D^{*-}_s)$	$[0.06, 0.07]$	$[-0.56, 0.69]$	

There are two RPV coupling products, $\lambda''^{*}_{231}\lambda''_{221}$ and $\lambda'^{*}_{i23}\lambda'_{i22}$, contributing to these exclusive $b \to c\bar{c}s$ decay modes at tree level. We use the experimental data listed in Eq. (33) to constrain the RPV coupling products, and the allowed spaces are shown in Fig. 4. The coupling $\lambda''^{*}_{231}\lambda''_{221}$ due to squark exchange contributes to all 12 relative decay modes. The allowed space of $\lambda''^{*}_{231}\lambda''_{221}$ is shown in the left plot of Fig. 4. The slepton exchange couplings $\lambda'^{*}_{i23}\lambda'_{i22}$ contribute to six $\bar{B}^0_d \to D^{(*)+}D^-_s$, $B^-_u \to D^{(*)0}D^-_s$, and $\bar{B}^0_s \to D^{(*)+}_s D^-_s$ decays, and the constrained space is displayed in the right plot of Fig. 4. From Fig. 4, we find that both moduli of RPV couplings have been limited as $|\lambda''^{*}_{231}\lambda''_{221}| < 8.05 \times 10^{-3}$ and $|\lambda'^{*}_{i23}\lambda'_{i22}| < 5.05 \times 10^{-3}$. Their RPV weak phases are not constrained much when their magnitudes are less than about 1×10^{-3}.

Next, using the constrained parameter spaces shown in Fig. 4, we are going to predict RPV effects on the observables which have not been measured yet. We summarize RPV MSSM predictions with two separate RPV coupling contributions in the last two columns of Tables V and VI.

The contributions of the $\lambda''^{*}_{231}\lambda''_{221}$ coupling due to squark exchange are summarized in the third columns of Tables V and VI. In Table V, we find that the ranges of all branching ratios are shrunk by the $\lambda''^{*}_{231}\lambda''_{221}$ coupling and the experimental constraints. In particular, $\lambda''^{*}_{231}\lambda''_{221}$ coupling effects could reduce the range of $\mathcal{B}(\bar{B}^0_s \to D^{*+}_s D^{*-}_s)$. However, the allowed ranges of three $f_L(B_{(s)} \to D^{*}_{(s)}D^{*}_s)$ and three $f_\perp(B_{(s)} \to D^{*}_{(s)}D^{*}_s)$ are enlarged by the $\lambda''^{*}_{231}\lambda''_{221}$ coupling. In Table VI, we can see that the $\lambda''^{*}_{231}\lambda''_{221}$ coupling does not affect $\mathcal{C}(\bar{B}^0_s \to D^{*+}_s D^-_s, D^{*+}_s D^-_s)$ much.

Meanwhile, RPV coupling effects could remarkably enlarge the allowed ranges of the other direct CPAs (about 10 times). Unfortunately, they are still too small to be measured at presently available experiments. It is interesting to note that mixing-induced CPAs of B_s decays are greatly affected by the $\lambda''^{*}_{231}\lambda''_{221}$ coupling. For example, $|\mathcal{S}(\bar{B}^0_s \to D^{(*)+}_s D^{(*)-}_s)|$ could be increased to $\sim$50% and their signs could be changed by the squark exchange coupling.

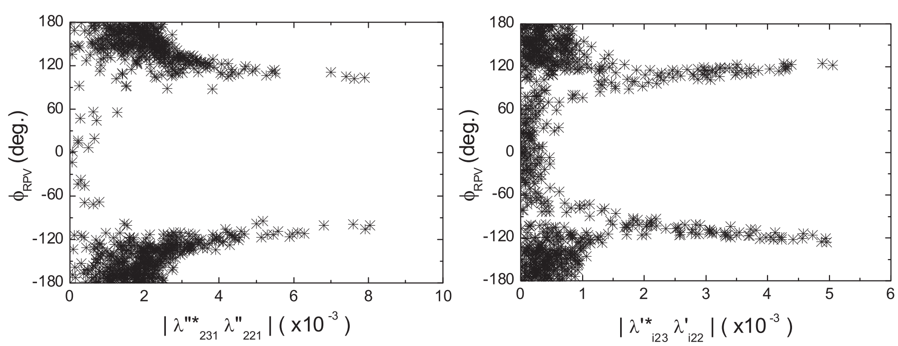

FIG. 4. Allowed parameter spaces for relevant RPV coupling products constrained by the measurements of the exclusive color-allowed $b \to c\bar{c}s$ decays listed in Eq. (33).

The contributions of $\lambda'^{*}_{i23}\lambda'_{i22}$ due to the slepton exchanges are listed in the last columns of Tables V and VI. From Table V, we find that the ranges of all branching ratios are shrunk by the $\lambda'^{*}_{i23}\lambda'_{i22}$ coupling and the experimental constraints. The last columns of Table VI show that the $\lambda'^{*}_{i23}\lambda'_{i22}$ coupling could enlarge the ranges of all the CPAs. Particularly, the $\lambda'^{*}_{i23}\lambda'_{i22}$ coupling could change the predicted $\mathcal{S}(B^0_s, \bar{B}^0_s \to D^{(*)}_s D_s)$ significantly from quite narrow SM ranges to $[-0.6, 0.6]$ or $[-1, 1]$. The upper limits of $|\mathcal{C}(B^0_s, \bar{B}^0_s \to D^{*+}_s D^-_s, D^+_s D^{*-}_s)|$ are increased a lot by $\lambda'^{*}_{i23}\lambda'_{i22}$ couplings.

Since RPV contributions to physical observables are also very similar in $\bar{B}^0_d \to D^{(*)+} D^{(*)-}_s$, $B^-_u \to D^{(*)0} D^{(*)-}_s$, and $\bar{B}^0_s \to D^{(*)+}_s D^{(*)-}_s$ systems, we show only a few observables of B_s decays as examples. Figures 5 and 6 show the variational trends in some observables with the $\lambda''^{*}_{231}\lambda''_{221}$ and $\lambda'^{*}_{i23}\lambda'_{i22}$ couplings, respectively.

First, we will elucidate the information implied in Fig. 5. From Fig. 5(a), we find that $\mathcal{B}(\bar{B}^0_s \to D^{*+}_s D^{*-}_s)$ is not changed much by $|\lambda''^{*}_{231}\lambda''_{221}|$ and could have only a small value when $\phi_{\rm RPV}$ is not too large. As shown in Fig. 5(b), $f_\perp(\bar{B}^0_s \to D^{*+} D^{*-}_s)$ is increasing with $|\lambda''^{*}_{231}\lambda''_{221}|$, and also could have a small value when $\phi_{\rm RPV}$ is small. From Figs. 5(c) and 5(d), we find that $|\mathcal{S}(B^0_s, \bar{B}^0_s \to D^+_s D^-_s, D^{*+}_s D^-_s)|$ are all rapidly increasing with $|\lambda''^{*}_{231}\lambda''_{221}|$ and could be very large at the large values of $|\lambda''^{*}_{231}\lambda''_{221}|$ and $|\phi_{\rm RPV}|$; furthermore, the RPV weak phase has opposite effects in $|\mathcal{S}(B^0_s, \bar{B}^0_s \to D^+_s D^-_s)|$ and $|\mathcal{S}(B^0_s, \bar{B}^0_s \to D^{*+}_s D^-_s)|$. $\lambda''^{*}_{231}\lambda''_{221}$ coupling effects on $\mathcal{S}(B^0_s, \bar{B}^0_s \to D^+_s D^{*-}_s)$ $[\mathcal{S}(B^0_s, \bar{B}^0_s \to D^{*+}_s D^{*-}_s)]$ are similar to the ones on $\mathcal{S}(B^0_s, \bar{B}^0_s \to D^{*+}_s D^-_s)$ $[\mathcal{S}(B^0_s, \bar{B}^0_s \to D^+_s D^-_s)]$. So any measurement of $\mathcal{S}(B^0_s, \bar{B}^0_s \to D^{(*)+}_s D^{(*)-}_s)$ in the future will strongly constrain the magnitude and RPV weak phase of the $\lambda''^{*}_{231}\lambda''_{221}$ coupling, and then other mixing-induced CPAs will be more accurately predicted, as indicated by Figs. 5(c) and 5(d). As shown in Fig. 5(e), $\mathcal{C}(B^0_s, \bar{B}^0_s \to D^+_s D^-_s)$ has similar trends as $\mathcal{S}(B^0_s, \bar{B}^0_s \to D^+_s D^-_s)$ with $|\lambda''^{*}_{231}\lambda''_{221}|$ and $\phi_{\rm RPV}$; however, $\lambda''^{*}_{231}\lambda''_{221}$ coupling effects on the former are much smaller than the effects on the latter. $\mathcal{A}^{\rm dir}_{CP}(B_{u,d} \to DD^-_s, D^*D^-_s, D^*D^{*-}_s)$ and $-\mathcal{A}^{\rm dir}_{CP}(B_{u,d} \to DD^{*-}_s)$ have the same variational trends with $\lambda''^{*}_{231}\lambda''_{221}$ as $\mathcal{C}(B^0_s, \bar{B}^0_s \to D^+_s D^-_s)$ has. $\mathcal{C}(B^0_s, \bar{B}^0_s \to D^{*+}_s D^-_s, D^{*+}_s D^-_s)$ decays are not affected much by the $\lambda''^{*}_{231}\lambda''_{221}$ coupling, and we show $\mathcal{C}(B^0_s, \bar{B}^0_s \to D^{*+}_s D^-_s)$ in Fig. 5(f) as an example.

Figure 6 illustrates $\lambda'^{*}_{i23}\lambda'_{i22}$ contributions to the CPAs of $\bar{B}^0_s \to D^{(*)+}_s D^-_s$. As displayed in Figs. 6(a) and 6(b), $\mathcal{S}(B^0_s, \bar{B}^0_s \to D^{(*)+}_s D^-_s)$ decays are very sensitive to $\lambda'^{*}_{i23}\lambda'_{i22}$ couplings. $|\mathcal{S}(B^0_s, \bar{B}^0_s \to D^{(*)+}_s D^-_s)|$ decays are strongly increasing with $|\lambda'^{*}_{i23}\lambda'_{i22}|$, and they could reach an extremum at $|\phi_{\rm RPV}| \approx 120°$. The $\lambda'^{*}_{i23}\lambda'_{i22}$ coupling effects on $\mathcal{S}(B^0_s, \bar{B}^0_s \to D^+_s D^{*-}_s)$ are the same as the ones

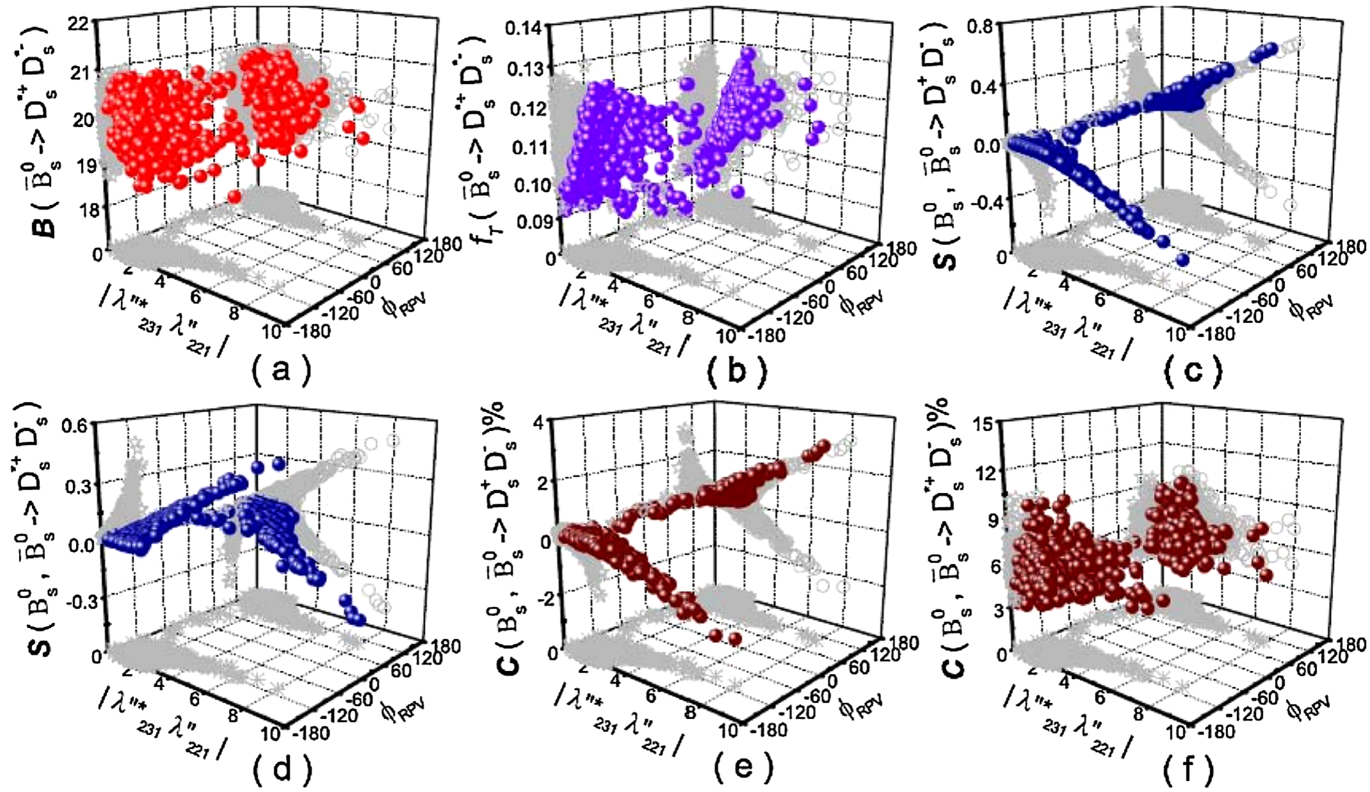

FIG. 5 (color online). Effects of the RPV coupling $\lambda''^{*}_{231}\lambda''_{221}$ on $\bar{B}^0_s \to D^{(*)+}_s D^{(*)-}_s$ decays, where $|\lambda''^{*}_{231}\lambda''_{221}|$ is in units of 10^{-3}, $\mathcal{B}$ is in units of 10^{-4}, and f_T denotes the transverse polarization fraction $f_\perp$.

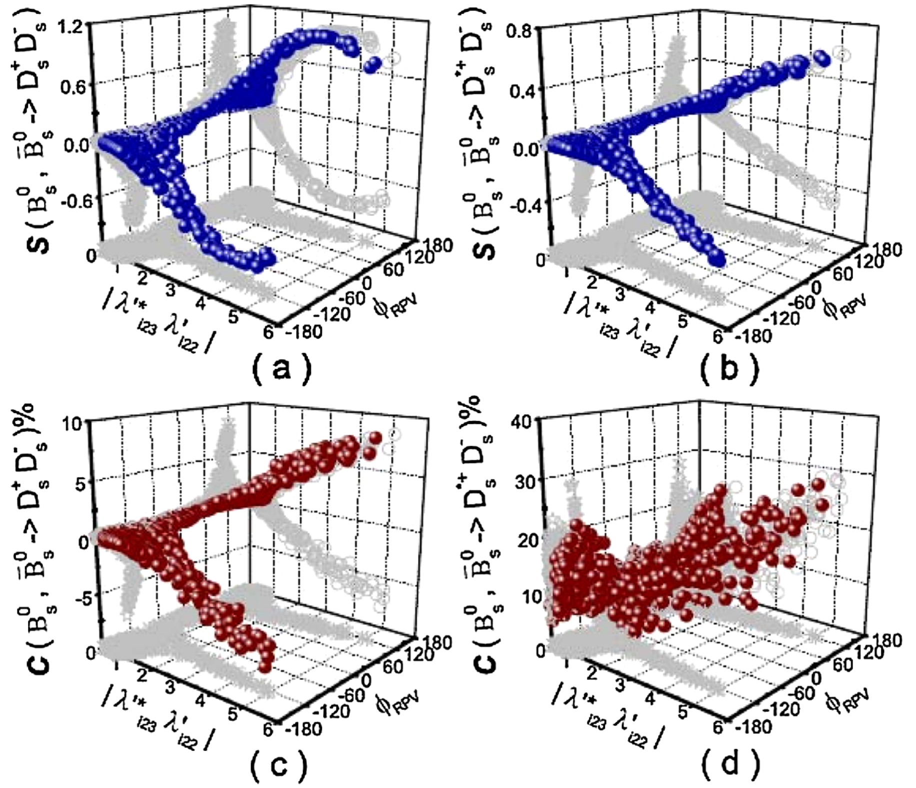

FIG. 6 (color online). Effects of $\lambda'^{*}_{i23}\lambda'_{i22}$ on $\bar{B}^0_s \to D_s^{(*)+}D_s^-$ decays, where $|\lambda'^{*}_{i23}\lambda'_{i22}|$ are in units of 10^{-3} and $\mathcal{B}$ in units of 10^{-4}.

on $\mathcal{S}(B^0_s, \bar{B}^0_s \to D_s^{*+}D_s^-)$. Figure 6(c) shows that $\mathcal{C}(B^0_s, \bar{B}^0_s \to D_s^+D_s^-)$ decays are also very sensitive to $|\lambda'^{*}_{i23}\lambda'_{i22}|$ and $\phi_{\rm RPV}$, but this is still too small to be measured in the near future. In addition, $\mathcal{A}^{\rm dir}_{CP}(B_{u,d} \to D^{(*)}D_s^-)$ decays are affected much by $\lambda'^{*}_{i23}\lambda'_{i22}$ couplings, and just the RPV MSSM predictions of these quantities are very small. $\lambda'^{*}_{i23}\lambda'_{i22}$ couplings could have a similar impact on $\mathcal{C}(B^0_s, \bar{B}^0_s \to D_s^{*+}D_s^-)$ and $-\mathcal{C}(B^0_s, \bar{B}^0_s \to D_s^{*+}D_s^-)$. We give the coupling effects on $\mathcal{C}(B^0_s, \bar{B}^0_s \to D_s^{*+}D_s^-)$ in Fig. 6(d), which shows that $\mathcal{C}(B^0_s, \bar{B}^0_s \to D_s^{*+}D_s^-)$ is increasing with $|\lambda'^{*}_{i23}\lambda'_{i22}|$ and could have a large value at large $|\phi_{\rm RPV}|$.

IV. SUMMARY

We have studied the 24 double charm decays $\bar{B}^0_d \to D^{(*)+}D^{(*)-}_{(s)}$, $B^-_u \to D^{(*)0}D^{(*)-}_{(s)}$, and $\bar{B}^0_s \to D_s^{(*)+}D^{(*)-}_{(s)}$ in the RPV MSSM. We have treated these decays in the naive factorization approximation and removed the known k^2 ambiguities in the penguin contributions via $b \to qg^*(\gamma^*) \to qc\bar{c}$ by calculating its hard kernel $b \to c + D_q$. Considering the theoretical uncertainties and the experimental error bars, we have obtained fairly constrained parameter spaces of RPV couplings from the present experimental data, which have very highly consistent measurements among the relative collaborations. Furthermore, using the constrained RPV coupling parameter spaces, we have predicted the RPV effects on the branching ratios, the CPAs, and the polarization fractions, which have not been measured or have not been well measured yet.

The investigation of exclusive color-allowed $b \to c\bar{c}d$ decays is motivated by the large direct CPA $\mathcal{C}(B^0_d, \bar{B}^0_d \to D^+D^-)$ reported by Belle, which has not been confirmed by *BABAR* yet and contradicted the SM prediction. Using the most conservative experimental bounds from $\bar{B}^0_d \to D^{(*)+}D^{(*)-}$ and $B^-_u \to D^{(*)0}D^{(*)-}$ systems (choose only 12 highly consistent measurements between *BABAR* and Belle), we have first obtained very strong constraints on the involved RPV couplings $\lambda''^{*}_{232}\lambda''_{212}$ and $\lambda'^{*}_{i23}\lambda'_{i21}$ from the $b \to c\bar{c}d$ transition, due to squark exchange and slepton exchanges, respectively. Then, using the constrained RPV coupling parameter spaces, we have predicted the RPV effects on $\mathcal{C}(B^0_d, \bar{B}^0_d \to D^+D^-)$ and other observables, which have less consistent measurements or have not been measured yet. We have found that the lower limit of $\mathcal{C}(B^0_d, \bar{B}^0_d \to D^{(*)+}D^-)$ could be slightly reduced by the RPV couplings. Our RPV MSSM prediction of $\mathcal{C}(B^0_d, \bar{B}^0_d \to D^+D^-)$ is consistent with *BABAR* measurements within the 1σ error level, but cannot explain the corresponding Belle experimental data within the 3σ level. We have also found that the contributions of $\lambda''^{*}_{232}\lambda''_{212}$ and $\lambda'^{*}_{i23}\lambda'_{i21}$ cannot affect the relevant branching ratios much. $\lambda''^{*}_{232}\lambda''_{212}$ or $\lambda'^{*}_{i23}\lambda'_{i21}$ contributions could greatly enlarge the ranges of the relevant mixing-induced CPAs $\mathcal{S}(B^0_d, \bar{B}^0_d \to D^{(*)+}D^{(*)-})$

from their SM predictions, and these quantities are very sensitive to the moduli and weak phases of $\lambda''^{*}_{232}\lambda''_{212}$ and $\lambda'^{*}_{i23}\lambda'_{i21}$. So, more accurate measurements of $\mathcal{S}(B^0_d, \bar{B}^0_d \to D^{(*)+}D^{(*)-})$ in the future will much more strongly constrain these RPV couplings, and then mixing-induced CPAs can be more accurately predicted as well. Effects of the $\lambda''^{*}_{232}\lambda''_{212}$ coupling could slightly extend the allowed regions of four $\mathcal{C}(B^0_d, \bar{B}^0_d \to D^{(*)+}D^{(*)-})$ and eight $\mathcal{A}^{\rm dir}_{CP}(B^-_u \to D^{(*)0}D^{(*)-}, \bar{B}^0_s \to D^{(*)+}_s D^{(*)-})$. $\mathcal{C}(B^0_d, \bar{B}^0_d \to D^{(*)+}D^-)$ decays are also sensitive to the slepton exchange couplings $\lambda'^{*}_{i23}\lambda'_{i21}$, and their signs could be changed by these couplings. Additionally, three $f_L(B_{(s)} \to D^*_{(s)}D^*)$ and three $f_\perp(B_{(s)} \to D^*_{(s)}D^*)$ are decreased and increased by the $\lambda''^{*}_{232}\lambda''_{212}$ coupling, respectively, and their allowed ranges are magnified by these couplings.

For $\bar{B}^0_d \to D^{(*)+}D^{(*)-}_s$, $B^-_u \to D^{(*)0}D^{(*)-}_s$, and $\bar{B}^0_s \to D^{(*)+}_s D^{(*)-}_s$ decays, the RPV couplings $\lambda''^{*}_{231}\lambda''_{221}$ and $\lambda'^{*}_{i23}\lambda'_{i22}$ contribute to these decay modes. We have found that $\lambda''^{*}_{231}\lambda''_{221}$ coupling effects could apparently suppress the upper limit of $\mathcal{B}(\bar{B}^0_s \to D^{*+}_s D^{*-}_s)$ and could slightly enlarge the allowed ranges of three $f_L(B_{(s)} \to D^*_{(s)}D^*_s)$ and three $f_\perp(B_{(s)} \to D^*_{(s)}D^*_s)$; nevertheless, these quantities are not very sensitive to the changes of $|\lambda''^{*}_{231}\lambda''_{221}|$ and $\phi_{\rm RPV}$. $\mathcal{C}(\bar{B}^0_s \to D^{*+}_s D^-_s, D^+_s D^{*-}_s)$ decays are evidently not affected by the squark exchange $\lambda''^{*}_{231}\lambda''_{221}$ coupling, and their upper limits are increased a lot by the slepton exchange $\lambda'^{*}_{i23}\lambda'_{i22}$ couplings. RPV couplings $\lambda''^{*}_{231}\lambda''_{221}$ and $\lambda'^{*}_{i23}\lambda'_{i22}$ could greatly enlarge all other CP asymmetries, which are also very sensitive to the relevant RPV couplings. However, the direct CPAs are still too small to be measured soon. We could explore RPV MSSM effects from the mixing-induced CPAs of B_s decays.

With the large amount of B decay data from *BABAR* and Belle, especially from LHCb in the near future, measurements of previously known observables will become more precise and many unobserved observables will be also measured. From the comparison of our predictions in Figs. 2, 3, 5, and 6 with near future experiments, one will obtain more stringent bounds on the product combinations of the RPV couplings. On the other hand, the RPV MSSM predictions of other decays will become more precise because of the more stringent bounds on the RPV couplings. The results in this paper could be useful for probing RPV MSSM effects, and will correlate with searches for direct supersymmetry signals at future experiments, for example, the LHC.

ACKNOWLEDGMENTS

The work of C. S. K. was supported in part by CHEP-SRC and in part by the KRF Grant funded by the Korean Government (MOEHRD), No. KRF-2005-070-C00030. The work of R.-M. W. was supported by the second stage of the Brain Korea 21 Project. The work of Y.-D. Y. was supported by the National Science Foundation under Contract No. 10675039 and No. 10735080.

[1] A. I. Sanda and Z. z. Xing, Phys. Rev. D **56**, 341 (1997).
[2] Z. z. Xing, Phys. Rev. D **61**, 014010 (1999), and references therein.
[3] S. Fratina *et al.*, Phys. Rev. Lett. **98**, 221802 (2007).
[4] J. Anderson *et al.* (*BABAR* Collaboration), arXiv:0808.1866.
[5] T. Aushev *et al.* (Belle Collaboration), Phys. Rev. Lett. **93**, 201802 (2004).
[6] B. Aubert *et al.* (*BABAR* Collaboration), Phys. Rev. D **76**, 111102 (2007).
[7] H. Miyake *et al.* (Belle Collaboration), Phys. Lett. B **618**, 34 (2005).
[8] K. Vervink, arXiv:0810.3167.
[9] B. Aubert *et al.* (*BABAR* Collaboration), Phys. Rev. D **73**, 112004 (2006).
[10] K. Abe *et al.* (Belle Collaboration), arXiv:0708.1668.
[11] G. Majumder *et al.* (Belle Collaboration), Phys. Rev. Lett. **95**, 041803 (2005).
[12] R. Zwicky, Phys. Rev. D **77**, 036004 (2008).
[13] R. Fleischer, Eur. Phys. J. C **51**, 849 (2007).
[14] M. Gronau, J. L. Rosner, and D. Pirjol, Phys. Rev. D **78**, 033011 (2008).
[15] P. Fayet, Nucl. Phys. **B90**, 104 (1975); Phys. Lett. **64B**, 159 (1976); **69B**, 489 (1977); **84B**, 416 (1979).
[16] K. Inoue, A. Komatsu, and S. Takeshita, Prog. Theor. Phys. **68**, 927 (1982); **70**, 330(E) (1983); H. Nilles, Phys. Rep. **110**, 1 (1984); H. Haber and G. Kane, Phys. Rep. **117**, 75 (1985).
[17] S. Weinberg, Phys. Rev. D **26**, 287 (1982).
[18] N. Sakai and T. Yanagida, Nucl. Phys. **B197**, 533 (1982); C. Aulakh and R. Mohapatra, Phys. Lett. **119B**, 136 (1982).
[19] See, for example, R. Barbier *et al.*, Phys. Rep. **420**, 1 (2005), and references therein; M. Chemtob, Prog. Part. Nucl. Phys. **54**, 71 (2005).
[20] B. C. Allanach *et al.*, arXiv:hep-ph/9906224, and references therein.
[21] G. Bhattacharyya and A. Datta, Phys. Rev. Lett. **83**, 2300 (1999); G. Bhattacharyya and A. Raychaudhuri, Phys. Rev. D **57**, R3837 (1998); R. Wang, G. R. Lu, E. K. Wang, and Y. D. Yang, Eur. Phys. J. C **47**, 815 (2006).
[22] A. Datta, Phys. Rev. D **66**, 071702 (2002); D. Chakraverty and D. Choudhury, Phys. Rev. D **63**, 075009 (2001); B. Dutta, C. S. Kim, and S. Oh, Phys. Lett. B **535**, 249 (2002); Phys. Rev. Lett. **90**, 011801 (2003).
[23] S. Nandi and J. P. Saha, Phys. Rev. D **74**, 095007 (2006);

Y. G. Xu, R. M. Wang, and Y. D. Yang, Phys. Rev. D **74**, 114019 (2006); C. S. Kim and R. M. Wang, Phys. Rev. D **77**, 094006 (2008); J. P. Saha and A. Kundu, Phys. Rev. D **66**, 054021 (2002).

[24] B. Dutta, C. S. Kim, S. Oh, and G. h. Zhu, Eur. Phys. J. C **37**, 273 (2004); Phys. Lett. B **601**, 144 (2004); Y. D. Yang, R. M. Wang, and G. R. Lu, Phys. Rev. D **72**, 015009 (2005).

[25] M. Wirbel, B. Stech, and M. Bauer, Z. Phys. C **29**, 637 (1985); M. Bauer, B. Stech, and M. Wirbel, Z. Phys. C **34**, 103 (1987).

[26] K. Abe *et al.* (Belle Collaboration), Phys. Rev. Lett. **89**, 122001 (2002).

[27] B. Aubert *et al.* (*BABAR* Collaboration), Phys. Rev. D **67**, 092003 (2003).

[28] B. Aubert *et al.* (*BABAR* Collaboration), Phys. Rev. D **74**, 031103 (2006).

[29] B. Aubert *et al.* (*BABAR* Collaboration), Phys. Rev. D **71**, 091104 (2005).

[30] S. Ahmed *et al.* (CLEO Collaboration), Phys. Rev. D **62**, 112003 (2000).

[31] D. Gibaut *et al.* (CLEO Collaboration), Phys. Rev. D **53**, 4734 (1996).

[32] D. Bortoletto *et al.* (CLEO Collaboration), Phys. Rev. D **45**, 21 (1992).

[33] D. Bortoletto *et al.*, Phys. Rev. Lett. **64**, 2117 (1990).

[34] H. Albrecht *et al.* (ARGUS Collaboration), Z. Phys. C **54**, 1 (1992).

[35] G. Buchalla, A. J. Buras, and M. E. Lautenbacher, Rev. Mod. Phys. **68**, 1125 (1996).

[36] M. Wirbel, B. Stech, and M. Bauer, Z. Phys. C **29**, 637 (1985).

[37] M. Neubert and V. Rieckert, Nucl. Phys. **B382**, 97 (1992).

[38] M. Gronau, Phys. Lett. B **233**, 479 (1989).

[39] J. Soto, Nucl. Phys. **B316**, 141 (1989).

[40] W. F. Palmer and Y. L. Wu, Phys. Lett. B **350**, 245 (1995).

[41] A. Ali, G. Kramer, and C. D. Lu, Phys. Rev. D **59**, 014005 (1998).

[42] W.-M. Yao *et al.*, J. Phys. G **33**, 1 (2006), and 2007 partial update for 2008, http://pdg.lbl.gov/.

[43] J. Charles *et al.* (CKMfitter Group), Eur. Phys. J. C **41**, 1 (2005); updated results and plots available at http://ckmfitter.in2p3.fr/.

[44] C. Aubin *et al.*, Phys. Rev. Lett. **95**, 122002 (2005).

[45] M. Neubert, Phys. Rep. **245**, 259 (1994).

[46] M. Neubert, Int. J. Mod. Phys. A **11**, 4173 (1996).

[47] M. Neubert, Phys. Rev. D **46**, 2212 (1992).

[48] H. Y. Cheng, C. K. Chua, and C. W. Hwang, Phys. Rev. D **69**, 074025 (2004).

[49] A. Zupanc *et al.*, Phys. Rev. D **75**, 091102 (2007).